INL/RPT-22-68628

Light Water Reactor Sustainability Program

Development and Demonstration of a Risk-Informed Approach to the Regulatory Required Fuel Reload Safety Analysis

August 2022

U.S. Department of Energy

Office of Nuclear Energy

INL/RPT-22-68628

Development and Demonstration of a Risk-Informed Approach to the Regulatory Required Fuel Reload Safety Analysis

Yong-Joon Choi[1]
Mohammad Abdo[1]
Gabrielle Palamone[2]
Stephen Heagy[2]
Cesare Frepoli[2]
Kingsley Ogujiuba[3]
Nicholas Rollins[3]
Gregory Deplipei[3]
Jason Hou[3]

[1]Idaho National Laboratory,
[2]FPoliSolutions LLC,
[3]North Carolina State University

August 2022

Prepared for the
U.S. Department of Energy
Office of Nuclear Energy
Under DOE Idaho Operations Office
Contract DE-AC07-05ID14517

Page intentionally left blank

EXECUTIVE SUMMARY

The United States (U.S.) nuclear industry is facing a strong challenge to maintain regulatory required levels of safety while ensuring economic competitiveness to stay in business. Safety remains a key parameter for all aspects related to the operation of light water reactor (LWR) nuclear power plants (NPPs) and can be achieved more economically by using a risk-informed ecosystem, such as the one being developed by the Risk-Informed Systems Analysis (RISA) Pathway under the U.S. Department of Energy (DOE) Light Water Reactor Sustainability (LWRS) Program. The LWRS Program is promoting a wide range of research and development (R&D) activities with the goal to maximize both the safety and economically efficient performance of NPPs through improved scientific understanding, especially given that many plants are considering second license renewal.

The RISA Pathway has two main goals: (1) the deployment of methodologies and technologies that enable better representation of safety margins and the factors that contribute to cost and safety; and (2) the development of advanced applications that enable cost-effective plant operation.

The plant reload optimization framework development project aims to build a reactor core designing tool that integrates reactor safety and fuel performance analyses and uses artificial intelligence to support optimization of core design solutions.

This report summarizes the following activities that were successfully performed in fiscal year (FY)-2022:

- Enhancement of a single objective genetic algorithm (GA)-based optimization framework by applying evolution, mutation, survivor, and constraints control methods.
- Investigation of new experiment data and water droplet models to improve uncertainty analysis in a reflood phenomenon during a loss of coolant accident (LOCA).
- Assessment of the applicability of the risk-informed methodology to the plant reload optimization framework.
- A comprehensive benchmark study for the core design and fuel performance computational tools to be used in a GA-based optimization framework.

Page intentionally left blank

CONTENTS

FIGURES

TABLES

ACRONYMS

1D	one-dimensional
2D	two-dimensional
3D	three-dimensional
ADF	assembly discontinuity factor
AFD	axial flux difference
AI	artificial intelligence
ANM	analytical nodal method
ANO-1	Arkansas Nuclear One Unit
ANSI	American National Standards Institute
AOO	anticipated operational occurrence
API	applied programming interface
ASPR	axial power shaping rods
ATF	accident tolerance fuel
BEPU	best estimate plus uncertainty
BOC	beginning of cycle
BWR	boiling water reactor
CAOC	constant axial offset control
CASL	Consortium for Advance Simulation of Light Water Reactors
CE	continuous energy
CMFD	coarse mesh finite difference
COLR	core operating limits report
CPU	central processing unit
CTF	COBRA-TF
CWO	core-wide oxidation
DBA	design basis accident
DNBR	departure nucleate boiling rate
DOE	U.S. Department of Energy
EOC	end of cycle
ESSM	embedded self-shielding method
FEBA	flooding experiments with blocked arrays
FOM	figure of merits
FSAR	final safety analysis report
FY	fiscal year

GA	genetic algorithm
HALEU	high assay low enriched uranium
HFP	hot full power
HPC	high-performance computing
HZP	hot zero power
IAEA	International Atomic Energy Agency
IFA	Instrumented Fuel Assembly
IFBA	Integral Fuel Burnable Absorber
IFPE	International Fuel Performance Experiment
INL	Idaho National Laboratory
ITU	Institute for Transuranium Elements
JRC	Joint Research Centre
LB	large break
LBE	licensing basis event
LBLOCA	large break loss of coolant accident
LCP	licensed core power
LEU	low-enriched uranium
LHR	linear heat rate
LOCA	loss of coolant accident
LTC	long-term cooling
LWR	light water reactor
LWRS	Light Water Reactor Sustainability
MLO	maximum local oxidation
MOC	Method of Characteristics
MOF	modular optimization framework
MTC	moderator temperature coefficient
NEA	Nuclear Energy Agency
NEI	Nuclear Energy Institute
NEM	nodal expansion method
NPP	nuclear power plant
NRC	U.S. Nuclear Regulatory Commission
NSGAII	non-dominated sorting genetic algorithm II
OECD	Organization for Economic Cooperation and Development
PCT	peak cladding temperature
PDF	probability density function

PRA	probabilistic risk assessment
PWR	pressurized water reactor
QPT	quadrant power tilt
R&D	research and development
RAOC	relaxed axial offset control
RAVEN	Risk Analysis and Virtual Environment
RBHT	rod bundle heat transfer
RCS	reactor coolant system
RELAP	Reactor Excursion and Leak Analysis Program
RIP	rod internal pressure
RIPB	risk-informed performance-based
RISA	Risk-Informed Systems Analysis
ROM	reduce order model
RPS	reactor protection system
RSAC	reload safety analysis checklist
RSE	reload safety evaluation
SB	small break
SBLOCA	small break loss of coolant accident
SDM	shutdown margin
SER	safety evaluation report
SRP	Standard Review Plan
TH	thermal-hydraulics
TRISO	tri-structural isotropic
TRL	technology readiness level
TVA	Tennessee Valley Authority
UQ	uncertainty quantification
U.S.	United States
WABA	wet annular burnable absorber
WBN1	Watts Bar Nuclear Unit 1
ZPPT	Zero Power Physics Test

1. INTRODUCTION

The United States (U.S.) Department of Energy (DOE) Light Water Reactor Sustainability (LWRS) Program Risk-Informed Systems Analysis (RISA) Pathway Plant Reload Optimization Project aims to develop an integrated, comprehensive framework offering an all-in-one solution for reload evaluations with a special focus on optimization of core design [1]. The optimization of the fuel loading pattern is one of the most important considerations in reducing the amount of new fuel used in the core. However, the loading pattern cannot be optimized by itself. Fuel performance analysis and system safety analysis (i.e., thermal-hydraulics) results also need to be considered to determine the most appropriate loading patterns. Due to thousands of possible options of core configuration, finding optimal solutions is an unachievable task for a human. However, it can be solved using modern artificial intelligence (AI) techniques.

Among various of AI-based methods, the Genetic Algorithm (GA) has been chosen as a basis of optimization framework. This GA method is a proven technology for fuel reload optimization purpose [2]. The following is the advantages from GA method:

- Can generate multiple solutions in relationship to the optimization problem so that it has maintained its reputation as a reference method in the loading pattern optimization fields.
- Does not require intrusive access to the physics being optimized; hence, they are great with black box models.
- Works with both convex and non-convex problems, as the results do not stick in local optima; this makes them one of the powerful global optimizers.
- Can handle both constrained and unconstrained problems

In this research, the chosen GA method and path relinking were coupled to scatter search, which shows the best results in terms of global cost [3]. In this regard, a modular optimization framework (MOF) was proposed to facilitate the application of other optimization methods, as well as the GA using object-oriented programming [4]. The Risk Analysis and Virtual Environment (RAVEN) [5] was utilized as a main controller, as well as the reloading pattern optimization framework. The modular way by which the algorithms are implemented in RAVEN facilitates the flexibility of dealing with discrete and continuous variables (i.e., integers, floats, and binary variables).

RAVEN's capability is not just limited to optimization but can also provide input decks to other physical codes and perform post-processing of the simulation results. This extensibility of RAVEN facilitates the coupling with other physical codes for core design, fuel performance, and systems analysis, which can lead to creating a unified framework considering physical phenomena. Hence, using RAVEN as a controller of GA method will give a highest benefit as a one-stop plant reload optimization framework which gives easy access to the users.

Previous efforts were focused on developing basic optimization framework based on GA method. An initial demonstration was performed to find an optimized PWR reactor core with maximum fuel operation length [1]. Fiscal year (FY)-2022 focused on improvement of GA method and uncertainty analysis and assessment of risk-informed methodology applicability to plant reload optimization framework. A comprehensive benchmark study was also performed to remove constraints in core design and fuel performance analysis computational tools.

Here are four major accomplishments in FY-2022:

- Enhancement of a single objective method GA-based optimization framework. Additional option models for the evolution, mutation, survivor, and constraints control methods were added to the RAVEN code. Coupling between RAVEN and core design and fuel performance codes are undergoing. Section 0 provides more details on these efforts.

- New experiment data were investigated to improve uncertainty analysis in reflood phenomenon during loss of coolant accident (LOCA). Flooding experiments with blocked arrays (FEBAs) was selected, and data is currently under review. The new droplet models were also identified to improve the uncertainty analysis. New models include different thermal-hydraulics (TH) characteristics from the parts of the fuel assembly. Section 3 summarizes the study results.
- The applicability of the risk-informed methodology to the plant reload optimization framework has been assessed. The major benefit of safety margin management from the risk-informed methodology can provide an enhanced licensing approach for accident tolerant fuel (ATF) and extended burnup operation. Section 3.2 describes the assessment outcome.
- A comprehensive benchmark study performed for the core design and fuel performance computational tools to be used in the GA-based optimization framework. The optimal tools were selected based on applicability to the GA-based plant reload optimization framework led by RAVEN. Details of the benchmark study are shown in Section 5 and Appendix A.

1.1 Objectives and Plan

The goal of this research is to develop an integrated, comprehensive framework offering an all-in-one solution for the reload evaluations with a special focus on optimization of fuel design [1]. The goal is to develop a framework that provides an optimized reactor core configuration based on key safety parameters that must be considered to meet regulatory requirements.

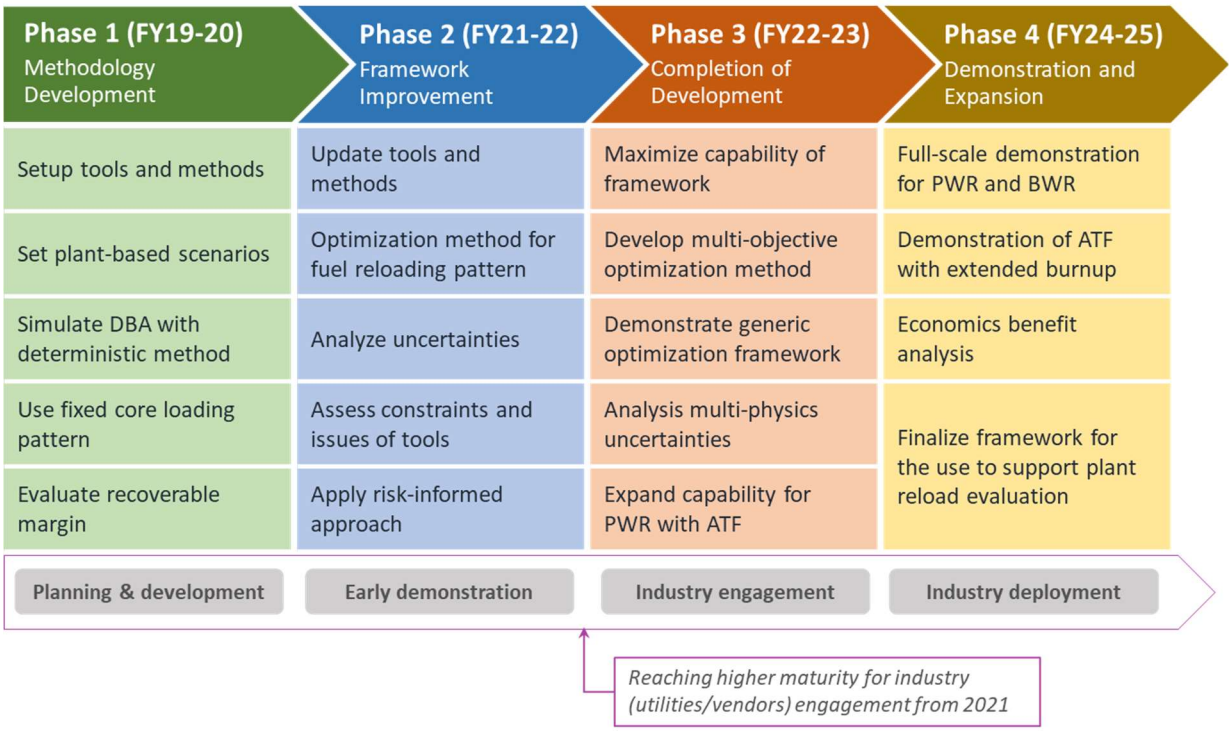

Figure 1-1. Technology roadmap of the Plant Reload Optimization Project.

Figure 1-1 shows the technology roadmap and research plan of this project throughout the last several FYs with four phases of research and development (R&D):

Phase 1 (FY-2019 to FY-2020): Methodology Development

Available tools and methods were investigated and tested. Plant-based design basis accident (DBA) scenarios were simulated via traditional deterministic methods by using the Reactor Excursion and Leak

Analysis Program version 5 (RELAP5)-three-dimensional (3D) [6] TH analysis code developed at Idaho National Laboratory (INL). Simulations used fixed core loading and evaluated recoverable margins [7].

Phase 2 (FY-2021 to FY-2022): Framework Improvement

Ten limiting DBA scenarios for a generic pressurized water reactor (PWR) and single objective optimization framework were developed. RAVEN infrastructure was improved for performance of neutronics and thermo-hydraulic analyses and tested with the reduced order model (ROM) to reduce computational burden. A best estimate plus uncertainty (BEPU) method was developed with improving the RELAP5-3D code and a LOCA event was simulated to identify uncertainties during the reflood phenomenon.

The research conducted over the last few years identified some constraints in the computational tools, especially in the field of reactor core design and fuel performance codes [1]. In FY-2022, the constraints in computational tools were reviewed through various benchmark studies. The applicability of the risk-informed approach for the plant reload optimization framework was assessed.

This study will be continued through the demonstration phase where the framework will be enhanced with additional and extended capabilities to support regulatory required fuel safety analyses. These extended capabilities will also address potential economic benefits from fuel reload optimization.

Phase 3 (FY-2022 to FY-2023): Completion of Development

Core design and TH tools will be tightly coupled to maximize the framework capability. The optimization method will be improved by further integration of the multi-objective GA method to complete a generic optimization framework development including multi-physics uncertainty analysis. Fuel reload optimization framework will be expand from the conventional zircalloy fuel to higher enriched ATF loaded PWR with extended burnup.

Phase 4 (FY-2024 to FY-2025): Demonstration and Expansion

The optimization framework capabilities will be expanded from PWR-centered core design to BWR. Full-scale demonstration for PWR and BWR will be performed. Economic benefits from using the plant reload optimization framework will be assessed to promote and expedite its deployment for industry use. While framework development will be finalized, and a pathway will be established to deploy it to industry where it could be used to support plant reload evaluations.

Upon finalizing the development, the following benefits will be obtained from the developed plant fuel reload optimization framework:

- This framework will significantly simplify the required process of core reload evaluation performed for each fuel reload because it integrates all required tasks into one seamless automated process.
- The framework will be capable to perform all necessary evaluations of ATF—including core design optimization.

2. DEVELOPMENT STATUS OF GA-BASED OPTIMIZATION FRAMEWORK

Traditional method of designing a reactor core rely on iterative method based on the knowledge of the expert. The reactor core design needs many of parameters to be considered: neutronics, fuel performance and TH modeling as well as to safety requirements and economics goal. Finding an optimized reactor core is very much labor intensive and costly. The reactor core design is in fact multi-physics and multi-scale problem which is a nonlinear problem that has no physical relation between the parameters of interest. Thus, it is not possible to develop a global model which can translate multi-physical input to safety requirements or economics outputs.

An alternative method was proposed inspired by Darwin's theory of evolution of species, the genetic algorithm [8]. Instead of solving physical problems, the GA method iterates group of potential solutions to find optimized solutions which meets user defined criteria. Since late 1990's GA method has been widely used in LWR core design, fuel management, and plant design as well as for the advanced nuclear system development [9].

The previous GA method optimization mostly limited to single-physics model. The RISA Pathway plant reload optimization framework, therefore, aims to develop a one-stop solution for multi-physic model including feedback from fuel performance and TH. The TH modeling also considers epistemic uncertainty in computational tools.

The GA-based optimization framework development progressed in FY-2022 by adding an option selection capability in the GA method procedure steps: fitness functions, parent selection, crossover, mutation, and survivor selection. The added options will significantly increase flexibility of the GA method by avoiding biased solutions which will allow more accurate results.

2.1 Demonstration of Single Objective GA Method

The definition of parameters used in GA method is inspired from biology [10]. The initial set of solutions—the population—has different solutions: (1) the chromosome, comprising the parameter of interest; (2) the gene; and (3) the value of the parameter, the allele. Figure 2-1 shows a schematic diagram of the population and its element. In this case, there are seven sets of potential solutions: Ch1–Ch7. Each set (e.g., the chromosome) has five parameters: G1–G5. The value of G1 in Ch2 is "2."

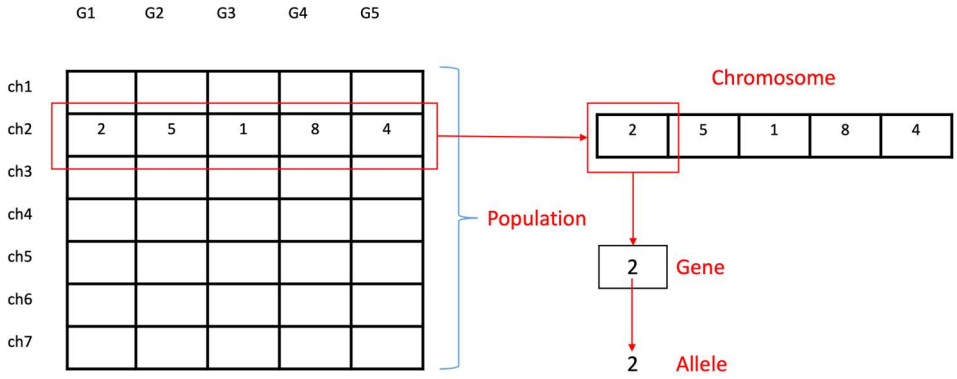

Figure 2-1. The set of potential solutions, the population, and elements of the solution for the chromosome, gene, and allele.

The user sets target criteria of the solution, i.e., fitness, and population is mixed from the first (e.g., the parent) to the second (e.g., the crossover) to the third (e.g., the mutation) generations. The potential

best solution (e.g., the survivor) is then assessed using the fitness criteria. If fitness criteria are met than it becomes to a final solution (e.g., the termination) or the population is repaired for a new iteration.

In FY-2021, core design optimization was demonstrated with a single objective, the maximum cycle length. The design goal of the optimization was the minimization of the fuel load. The performance goals were: (1) desired cycle length; and (2) minimizing the radial and axial power peaking. Additional performance goals were set as safety constraints from fuel performance analysis results, such as maximum oxidation or soluble boron concentration. The objective function was set to the maximization of the cycle length to meet the design goal, which is minimizing the amount of new fuel required to be used to meet the performance goals. To find an optimum core configuration (e.g., the chromosome), the population size was set to be 100, with 40 parents included in the mating pool. Options used for each step of the GA method is given in Table 2-1. The demonstration results showed about 600 days of maximum cycle [1].

Table 2-1. Options used at each step of GA method.

GA Step	Selected Options for Initial Demonstration
Fitness Evaluation	invLinear function.
Parent Selection	Roulette wheel.
Crossover	One-point crossover– (80% crossover probability with randomly chosen crossover location).
Mutation	Swap mutation– (90% mutation probability with randomly chosen mutation location).
Survivor Selection	Fitness-based survivor selection.
Termination Criteria	1) Maximum number of iterations. 2) *p-averaged* Hausdroff distance between two consecutive generations.

2.2 Implementation of the Options in GA Method Step

As shown in In FY-2021, core design optimization was demonstrated with a single objective, the maximum cycle length. The design goal of the optimization was the minimization of the fuel load. The performance goals were: (1) desired cycle length; and (2) minimizing the radial and axial power peaking. Additional performance goals were set as safety constraints from fuel performance analysis results, such as maximum oxidation or soluble boron concentration. The objective function was set to the maximization of the cycle length to meet the design goal, which is minimizing the amount of new fuel required to be used to meet the performance goals. To find an optimum core configuration (e.g., the chromosome), the population size was set to be 100, with 40 parents included in the mating pool. Options used for each step of the GA method is given in Table 2-1. The demonstration results showed about 600 days of maximum cycle [1].

, there are additional options in every step of the GA method to provide a more accurate random selection of potential solutions; these options were implemented into the RAVEN code.

2.2.1 Options in Fitness Evaluation Function

The notion of fitness is simple, but crucial, as it is the only way to judge if a chromosome, individual, and solution is good enough to be kept or discarded. In addition, it is the criteria that decides at the end of the iterations which candidate is the best solution. In the GA implementation in RAVEN, the fitness is flexible enough to allow the user to develop his/her own fitness function based on the nature of the model or black-boxed phenomenon being optimized. The requirements of the fitness function are:

- Efficiently implemented (e.g., it should never be the bottleneck of the algorithm).

- It should be maximum at the optima (e.g., for minimization problems: as the objective function decreases, the fitness should increase, and vice versa, whereas for the maximization problems, as the objective function increases, the fitness should also increase).
- The fitness should decrease whenever the constraints are violated (e.g., if it is a fitness that handles constraints).

Two different fitness functions are now available: (1) linear inverse fitness; and (2) feasible first.

2.2.1.1 Linear Inverse Fitness

This algorithm defines the fitness function as a linear combination of the objective function and the penalty generated if the chromosome violates the constraints.

2.2.1.2 Feasible First

This algorithm facilitates the handling of implicit and explicit constraints by additionally penalizing the violating chromosome by shifting it beyond the worst objective in the population.

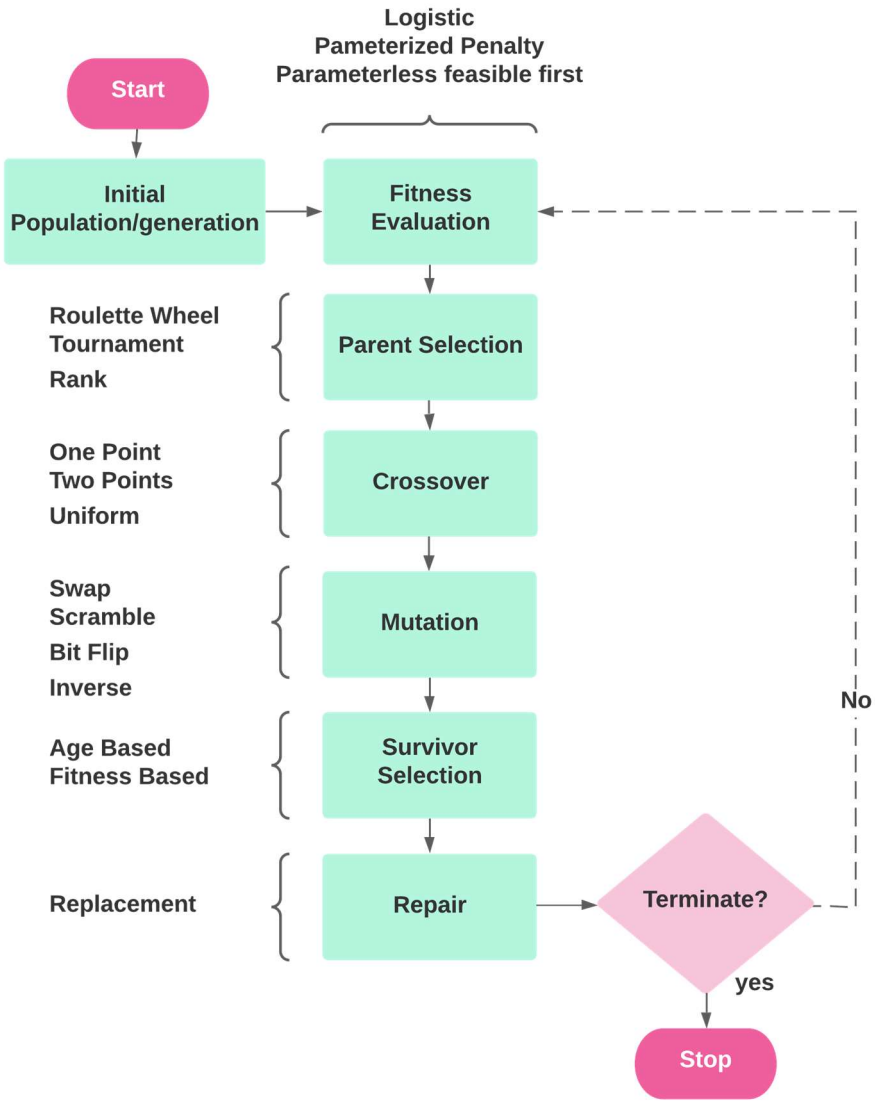

Figure 2-2. GA method flow chart.

2.2.2 Options in Parent Selection

Three different parent selection methods are now available to elect the elitist parents that will contribute to the reproduction (mating) process to generate next generation off-springs.

2.2.2.1 Roulette Wheel Method

In this algorithm, a random number is chosen on a wheel representing the relative fitness of a parent that is determined by the ratio of individual fitness and total fitness of the parent. That random number is then used for selecting each of the parents for the next generation of the experiment. The randomness assures that the highest fitness parent will not continue to be selected even if it represents the largest area allowing for escape from the local optima. The assurance of random selection of parents is important because it maximizes chances of finding the most optimal solution(s). Otherwise (i.e., if the selection is "stuck"), the solutions will be selected based on sampling from a limited pool with a chance to miss optimal solutions that are outside of that selection pool.

2.2.2.2 Tournament Selection

In this algorithm, a tournament based on fitness is held between each pair of parents and the more fit parent is selected until the required number of parents (e.g., *nParents*) is reached. Those remaining parents then represent the ones that contribute to the mating pool to create the new off-springs.

2.2.2.3 Rank Selection

In this algorithm, a ranking of all individuals in the population based on fitness is carried out and the top *nParents* are selected.

2.2.3 Options in Crossover

Three options are available in the crossover step: (1) one-point crossover; (2) two points crossover; and (3) uniform crossover.

2.2.3.1 One-Point Crossover

In the one-point crossover, a random crossover point is selected and the tails of its two parents are swapped to get new off-springs, as observed in Figure 2-3.

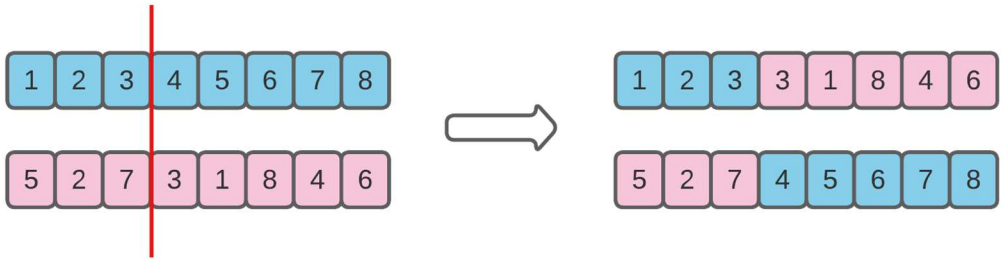

Figure 2-3. Schematic of the one-point crossover.

2.2.3.2 Two Points Crossover

Two points crossover is a generalization of the one-point crossover wherein alternating segments are swapped to get new off-springs, as shown in Figure 2-4.

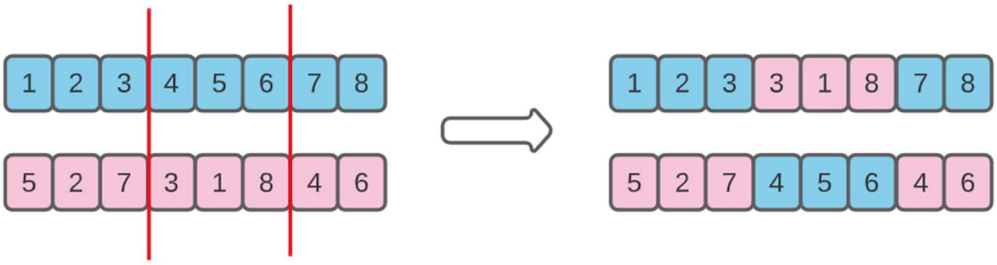

Figure 2-4. Schematic of the two points crossover.

2.2.3.3 Uniform Crossover

In a uniform crossover, the chromosome is divided by each gene separately. Each gene will be evaluated to decide whether to mix or not. Biasing to one parent is also possible to have more genetic material in the child from that parent, as observed in Figure 2-5.

Figure 2-5. Schematic of the uniform crossover.

2.2.4 Options in Mutation

Four options are now available to mutate genes in the resulting 'children' to allow for random genetic enhancements, which in turn prevent from getting stuck in local minima/valleys. These options are: (1) swap mutation; (2) scramble mutation; (3) bit flip mutation; and (4) option in repair.

2.2.4.1 Swap Mutation

In the swap mutation, two positions are selected on the chromosome at random with an interchange in the values, as can be seen in Figure 2-6.

Figure 2-6. Schematic of the swap mutation.

2.2.4.2 Scramble Mutation

In this mutation, a subset of genes is chosen from the entire chromosome and their values are scrambled or shuffled randomly, as observed in Figure 2-7.

Figure 2-7. Schematic of the scramble mutation.

2.2.4.3 Bit Flip Mutation

The bit flip mutation selects one or more random bits and then flips them, as shown in Figure 2-8. This method is dedicated for the mutation of the binary variables, thus, true or false, or, 1 or 0 by flipping the value to each other.

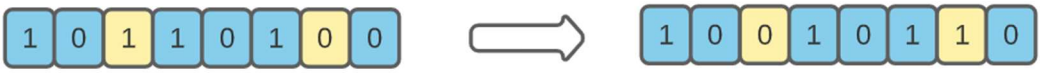

Figure 2-8. Schematic of the bit flip mutation.

2.2.4.4 Inversion Mutation

Inversion mutation selects a subset of genes as in the scramble mutation, but instead of shuffling the subset, the entire string in the subset is merely inverted, as shown in Figure 2-9.

Figure 2-9. Schematic of the inversion mutation.

2.2.5 Option in Repair

The crossover and mutation can alter the genetic aspects to violate some of the defined requirements, such as repeating the value of a gene in a problem that does not allow repetition. In similar cases, the algorithm has to take an action to repair the corrupted child. One option is available in the repair step.

2.2.5.1 Replacement Repair

In this algorithm, the undesirable genetic feature is randomly changed for that gene, which is withdrawn from the associate user-defined distribution, until the violation no longer exists.

2.2.6 Options in Survivor Selection

After the crossover, mutation and repair forged the genetic aspects of the new off-springs, and because of the randomness in these evolutionary operations, the fitness of the newly born children (e.g., solution candidates) should be evaluated and compared to other individuals/chromosomes in the population to make sure that what remains in the population for the next generation comprises stronger candidates than previous ones. There are two algorithms to perform such an important decision namely fitness-based survivor selection and age-based survivor selection.

2.2.6.1 Fitness-Based

In this fitness-based selection, the children tend to replace the least fit individuals in the population. The selection of the least fit individuals may be done using a variation of any of the selection policies described before (e.g., tournament selection, fitness proportionate selection, etc.).

For example, as shown in Figure 2-10, the children replace the least fit individuals P1 and P10 of the population. It is to be noted that since P1 and P9 have the same fitness value, the decision to remove which individual from the population is arbitrary.

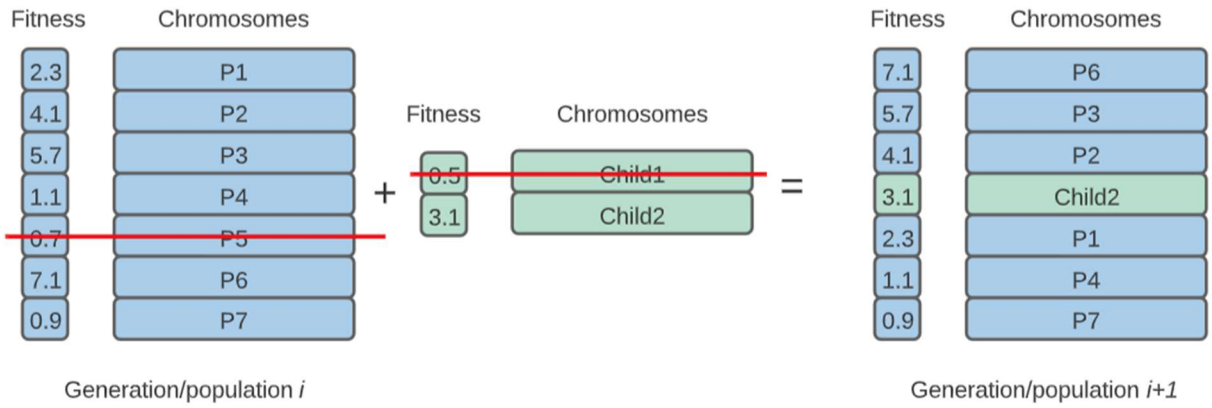

Figure 2-10. Schematic of the fitness-based survivor selection.

2.2.6.2 Age-Based

In this algorithm, a user-defined maximum age is used to discard any parent that has reached the maximum age, the age of an individual reflects how many generations that parent has survived. For instance, if the user selects an age of 'three' that means the individual that has survived for three generations will be eliminated, even if its fitness is still greater than some of the newly born children. This again prevents being stuck with the same individual/solution for many iterations.

As shown in Figure 2-11, the age is the number of generations for which the individual has been in the population. The oldest members of the population (i.e., P4 and P7) are removed and the ages of the rest are incremented by one.

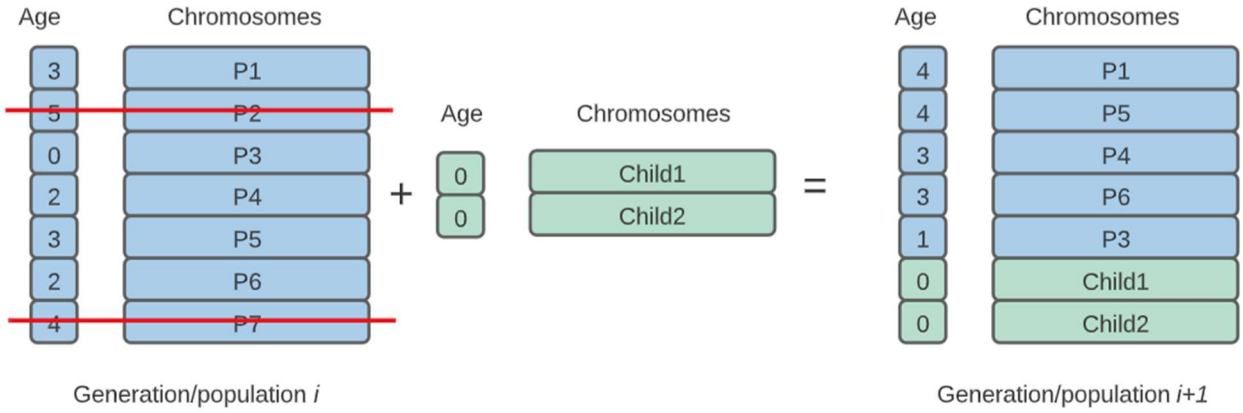

Figure 2-11. Schematic of the age-based survivor selection.

2.2.7 Options in Constraint Handling

Three constraint handling options are available: (1) box constraints; (2) explicit constraints; and (3) implicit constraints.

2.2.7.1 Box Constraints

Also known as boundary constraints, these define the upper and lower bounds of each gene/variable. In fact, these are actually handled out of the optimizer by the used-defined distributions. The user defines the type of the distribution associated with each variable, as well as the upper and lower bounds if finite. This prevents the optimizer from searching out these boundaries.

2.2.7.2 Explicit Constraints

Explicit constraints are functional constraints involving genes/input variables only.

2.2.7.3 Implicit Constraints

Implicit constraints are functional constraints involving genes/input variables, objective variables, and dependent variables. Both explicit and implicit constraints are converted to the form $g(\boldsymbol{x})>0$ for explicit constraints and $g(\boldsymbol{x},\boldsymbol{y})$ for implicit constraints where $\boldsymbol{x}$ is the input vector and $\mathbf{y}$ is a vector of output or dependent variables. If function g is smaller than zero, this flags a constraint violation that will be penalized in the fitness calculation as shown above.

2.3 Remarks and Future Works

The GA implementation in RAVEN relies on associating each gene/variable to a distribution. The GA can handle all sorts of variables, integers, floats, binary, and even a mix and match between them, rendering RAVEN the only open-source code that can deal with such difficult generalizations.

The distribution guides of the mutation and crossover operations, for instance, in the swap mutation of the genes are not simply swapped because each of the genes can come from a different distribution with a completely different meaning, one variable can be an angle while another can be a speed or fuel identification. In that case, swapping the values do not make any sense, but the probability distribution is swapped and the chosen value having the probability from the associated distribution of that variable remains. Again, this is an extremely rare quality that is unique to this development.

The discrete distribution can allow sampling with or without a replacement strategy allowing/forbidding the repetition of similar values, respectively. In some applications, the inventory of fuel pins requires repeating certain fuel pins a certain number of times because it is available in the inventory, this is handed as a constraint.

Future works planned for FY-2023 include maximizing the optimization framework capability to improve outcome quality and to perform full-scale demonstration:

- Verification and validation as well as unit and regression tests will be conducted. These tests will use a series of problems: (1) the Beale problem [11]; (2) the Mishra bird constrained problem [12]; (3) the Rosebrock [11], Simionescu [13], and Townsend problem [14]; and (4) the knapsack problem [15]. Every single mutation or crossover algorithm will also be tested with a unit test to compare the output to the expected output.
- Multi-objective optimization will be implemented for a realistic optimization demonstration. The non-dominated sorting genetic algorithm II (NSGAII) [16] will be used for the already developed Pareto Frontier concept.
- For demonstration purposes, RAVEN will be coupled with CASMO/SIMULATE [17] for the core design and TRANSURANUS [18] for fuel performance for the full-scale demonstration.

3. IMPROVEMENT OF UNCERTAINTY QUANTIFICATION METHODOLOGY

The plant reload optimization framework mainly uses a deterministic approach and eventually aims to apply fuel performance and TH feedback for the core design. Accurate (e.g., less conservative) feedback will demonstrate increased safety margin .

The major feedback from the systems analysis is the fuel failure sequences in the accident scenarios. As shown in Figure 3-1, the peak cladding temperature (PCT) occurs during the reflood phase and can lead fuel damage by plastic deformation (i.e., swelling) and fuel burst during a large break loss of coolant accident (LBLOCA) [19]. The radioactive materials in the fuel rod will be released into primary coolant system and then can be released into the containment and environment during a severe accident. Hence, an accurate analysis is necessary for the reflood phase. However, modeling of the reflood phase is very complicated due to the quick temperature drop (i.e., quenching). For this reason, the uncertainty quantification (UQ) in the reflood phase is considered the top priority in NPP accident analyses.

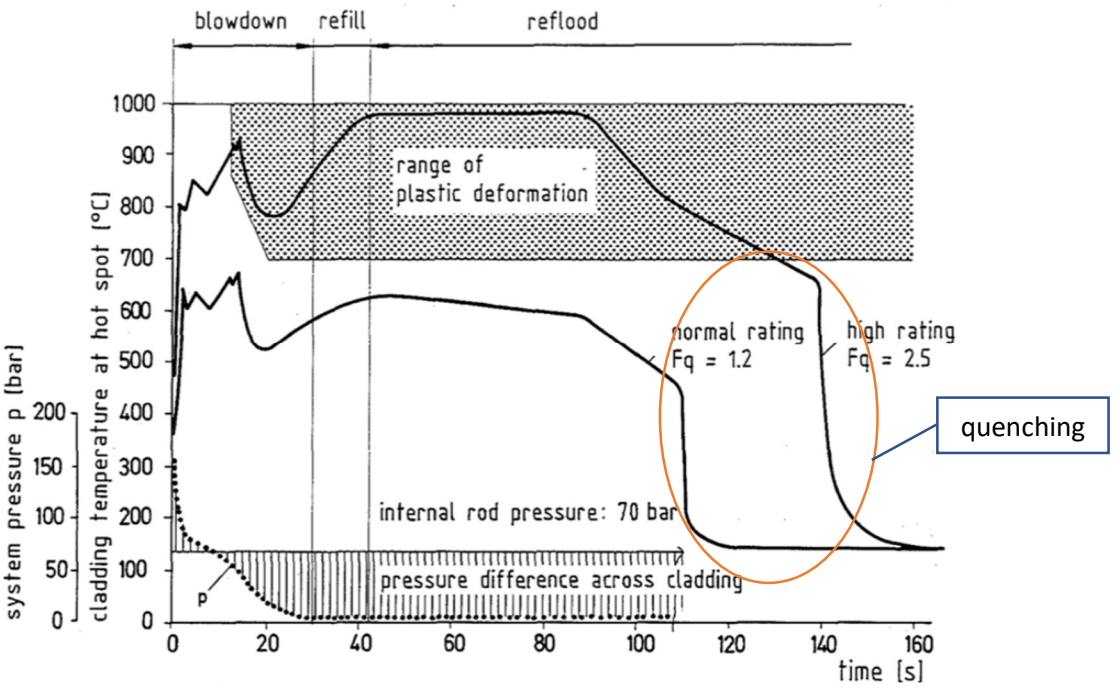

Figure 3-1. A generic description of the Zr fuel rod response during a double-ended cold leg break LOCA [19].

The BEPU method combines UQ and the best estimate analyses from the TH code RELAP5-3D. The BEPU method requires the following three applications: (1) UQ methods; (2) determination of the probability density functions (PDFs) for the input parameters; and (3) propagation of these PDFs through the RELAP5-3D simulations. This will derive the PDF of the figure of merits (FOMs).

In FY-2020 to FY-2021, RELAP5-3D was updated to include capabilities for perturbing relevant modeling parameters invoked by the code during the reflood phase of a LBLOCA simulation [20] and [21]. Those capabilities were implemented through the improvement of the RELAP5-3D source code to introduce PDF multipliers for perturbing the models' main parameters and to allow direct uncertainty propagation.

The PDF multipliers are based on experimental data and their accuracy can be improved as more experimental data are collected and applied. As a first test case, the FLECHT-SEASET experiments [22]

data were used for setting PDF multipliers. The RAVEN/RELAP5-3D coupled code was used and demonstrated the possibility of obtaining uncertainty bands and assessing the importance of different models influencing the FOMs. Figure 3-2 shows an example of results from the RELAP5-3D UQ for the FLECHT-SEASET test.

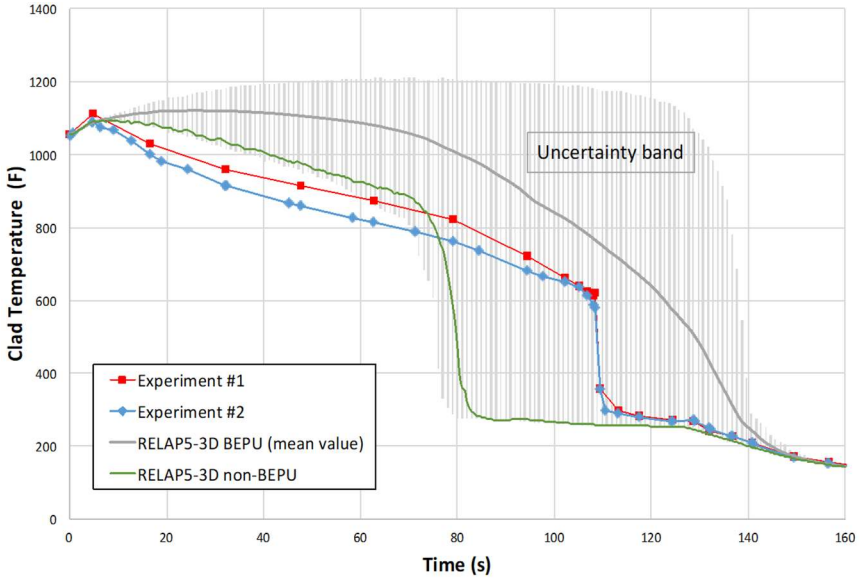

Figure 3-2. UQ of the FLECHT-SEASET test and comparison with the non-BEPU simulation.

In FY-2021, uncertainties in the LBLOCA analysis for Zion nuclear power plant (NPP) were analyzed by using MULTID component model in RELAP5-3D [1]. This model supports more accurate modeling of multi-dimensional hydrodynamic features of the reactor vessel (e.g., core, downcomer) and steam generator. The multi-dimensional component defines one-dimensional (1D), two-dimensional (2D), or three-dimensional (3D) array of volumes and the internal junctions connecting the volumes. The geometry can be either Cartesian or cylindrical. An orthogonal, 3D-grid was defined by mesh interval input data in each of the three coordinate directions. The MULTID model also allows to add the full momentum flux terms, as well as the associated input processing and checking. Figure 3-3 shows maximum cladding temperature comparison between the results shown in the final safety analysis report (FSAR) and RELAP5-3D results with an uncertainty band.

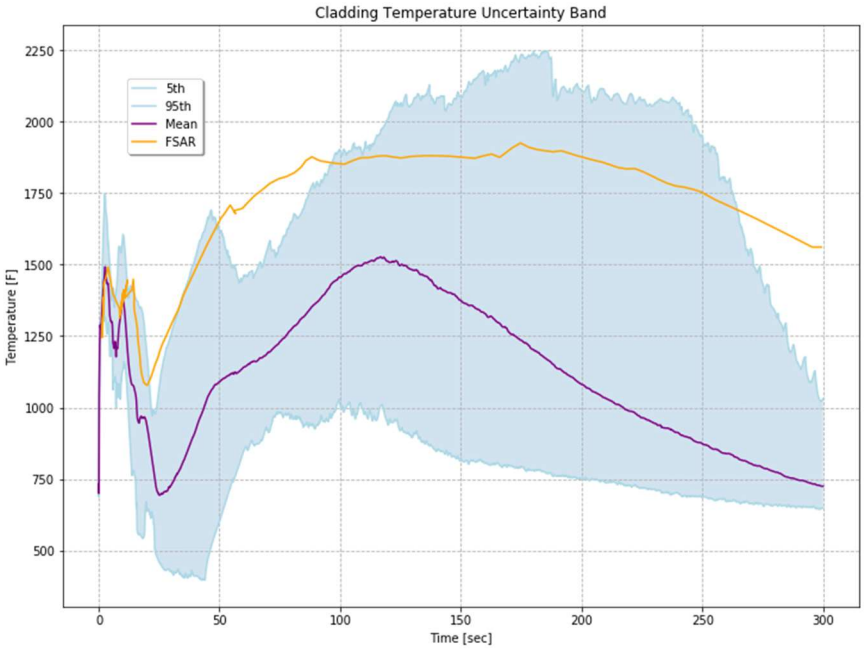

Figure 3-3. Maximum clad temperature and uncertainty band during LBLOCA in Zion NPP.

The current MULTID model uses interfacial friction multiplier as a global value for the entire component. During the research in FY-2021, it was found that this multiplier needs to be isolated for MULTID use to improve the model accuracy. The MULTID model also needs refinements in the vessel model for both axial and radial directions by allowing dense meshes. The following issues are still outstanding and should be taken into consideration with future updates which can provide more accurate simulation results which may allow to demonstrate larger safety margins:

- The lower plenum nodalization should be studied for the effects on fluid retention during LBLOCA blowdown.
- The downcomer nodalization should be studied for the effects on the emergency core cooling system bypass.
- The core and upper plenum modeling should be redesigned considering both the upper plenum structures above each fuel assembly and for handling power variation in assemblies.
- Components should be added or modified to properly model core bypass flow.

3.1 Improvement of Reflood Uncertainties

The accuracy of PDF multipliers can be improved by sufficient experimental data. The current UQ capability of RELAP5-3D is limited to FLECHT-SEASET test data. In FY-2022, the experimental data from the FEBA separate effect facility was selected for reflood data retrieval[1]. The experiments were performed in Germany in the 1980s to provide an independent source of reflood experimental data in a LBLOCA scenario for a PWR [23]. The database retrieval involved the execution of several scripts that converted and parsed the binary database in an ASCII format. The scope of using FEBA is to provide an independent set of reflood data for verifying and/or adjusting the guessed probability distribution functions of the identified closure laws parameters used for the FLECHT-SEASET tests.

The specific objectives of the separate effect tests under forced reflood conditions were:

[1] In the future, Rod Bundle Hat Transfer (RBHT) test data [27] will be also applied for the UQ analysis.

- To measure and evaluate TH data for unblocked rod bundle geometries
- To measure and evaluate the effects of grid spacers upon the TH behavior
- To measure and evaluate TH data for blocked bundle geometries with and without bypass.

Figure 3-4 shows the measured cladding temperature, fluid temperature, and heat transfer coefficient relative to the saturation temperature corresponding to the system pressure at an elevation of 590 mm close to the top end of heated bundle length for a test with a low flooding velocity of 2.2 cm/s and a system pressure of 4.1 bar. In much of the initial period of reflooding, the temperature of the vapor is higher than that of the cladding; consequently, the convective heat transfer is actually from the superheated steam to the cladding instead of the measured overall loss of heat from the cladding to the dispersed flow. The only exception to this is that at the very beginning, the measured heat transfer is indeed from the flow to the cladding as expected. This discrepancy in much of this period excluding the very beginning can be attributed to the effect of evaporative cooling of the smaller droplets in the flow most likely due to the presence of the grid spacers in the subchannel.

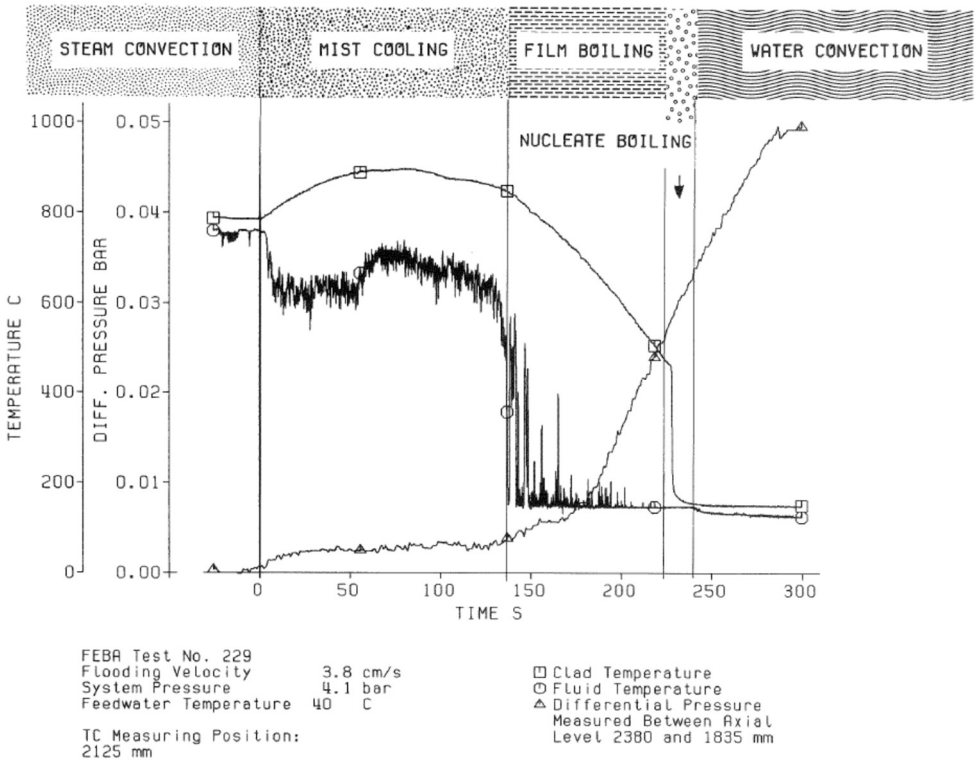

Figure 3-4. Cladding and fluid temperatures and heat transfer coefficient of the 5×5 rod bundle test.

The major conclusions of the FEBA experiments are:

- The cooling capacity of PWR fuel rod clusters blocked up to 90% is not a severe reflood cooling issue even for flooding velocities as low as 2 cm/s.
- Lower blockage ratios (e.g., 62%) lead to lower cladding temperatures in the blocked region than in unblocked rod clusters.
- Grid spacers increase the dispersed flow cooling effectiveness of the early portion of the reflood phase significantly.
- The results of the systematical investigations provide data for computer code model development and assessment concerning the blockage and grid spacer effects during reflooding PWR cores.

In FY-2023, the reflood phase UQ in RELAP5-3D will be improved by adding data from the FEBA facility. The rod bundle will be modeled using a PIPE component of RELAP5-3D with branches and time-dependent junctions for modeling the not-heated parts and the boundary conditions. The model will be coupled with RAVEN code for performing non-parametric Monte Carlo analyses.

3.2 Water Droplet Model Improvement

The fuel rod temperature behavior in a reflood phase is under the dispersed film boiling regime where peak cladding temperature occurs, which is critical to safety analysis. The generated water droplets from the film boiling generally vaporizes, collides, and merges, as well as breakup by the fuel assembly structure (e.g., spacer grid) and aerodynamic force, which the droplet diameter may change. However, RELAP5/Mod3.3, as well as RELAP5-3D, uses an average droplet diameter based on the total mass flux [24], along with the limiting conditions to avoid unrealistic results [25]. This method produces additional epistemic uncertainties during LOCA analyses.

Recent research developed a model to determine the mean diameter (i.e., Sauter mean diameter) by considering the mechanism of droplet size variation [26]. The water droplets in reflood phase are generally produced from water shattering and film detachment during the boiling in a dispersed film boiling regime. The size of the droplets changes due to various mechanical reactions. The new water droplet model accounts for the diameter change due to vaporization, breakup by spacer grid, and aerodynamic breakup. Developed new water droplet models were validated by using rod bundle heat transfer (RBHT) experiment [27].

Figure 3-5 shows the Sauter mean diameter at 2.9 m elevation and cladding temperature at 3.444 m elevation comparing the original version of RELAP5/Mod3.3, modified droplet model, and experimental data. It is clear that the modified model is more agreeable with the experiment. The cladding temperature simulation results show improvements for the entire duration of the simulation.

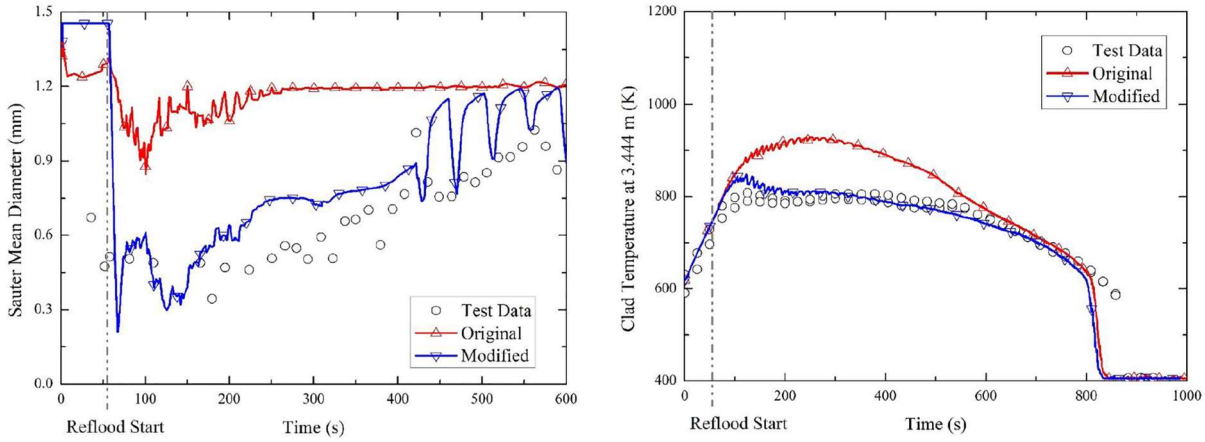

Figure 3-5. Sauter mean diameter (left) and cladding temperature (right) comparison.

This water droplet model will be applied to RELAP5-3D in the future to improve the modeling accuracy of the reflood phase which will provide better feedback to the core optimization framework.

4. APPLICABILITY ASSESSMENT OF THE RISK-INFORMED METHODOLOGY

Different trends in the industry suggest a technology-neutral methodology for performing the reload safety analysis and optimization of the core design to yield cost reduction would be of value. Among the drivers, the following are identified:

- ATFs, fuels with higher burnup, a higher enrichment of low-enriched uranium (LEU+) and high assay LEU (HALEU), and longer fuel cycles (from 18 to 24-months) have been considered by the industry.
- ATF holds the promise of enhancing safety at U.S. NPPs by offering better performance during normal operation, transient conditions, and accident scenarios, but current regulatory limits were designed for zircaloy-based fuel technologies.
- Utilities would benefit from performing core design independently in the direction to commoditize fuel supply. Fuel transition costs are deemed too high.

10 CFR 50.46 specifically calls out UO_2 and Zircaloy-based cladding in the regulation. In order to extend this regulation to other cladding types such as those being proposed for use in ATFs, rulemaking will need to occur to remove these specificities. Note that 10 CFR 50.46 acceptance criteria are really 'surrogate' to fuel failure mechanisms. Ultimately, the rule is ensuring that: (1) a core coolable geometry is maintained; (2) radioactivity release due to core damage is prevented; and (3) hydrogen generation and subsequent detonation (e.g., catastrophic failure) does not occur.

Even if utilities still deem that it is more effective to rely on a specific fuel vendor or in-house licensed method to optimize their core design, an alternative method could provide the value at least as an audit tool. More importantly, the rulemaking process needs to be better-informed by investigating the impact of a new fuel product (e.g., ATF, a new vendor, cycle length change, etc.) by realistically evaluating the risks of events to be considered. The recent advancements in the non-LWR licensing strategies that are based on frequency-consequence analyses could be leveraged to some extend to support licensing of different types of fuel for existing reactors.

4.1 Industry Methodology for Acceptable Cycle Reload Analyses

A literature review was performed to define industry practice at a high level when dealing with the core design. The review was limited at this time to PWR reactors but can be easily extended to BWRs in the future.

AREVA[2] methodology for cycle reload analyses provides a good example [28]. Figure 4-1 provides the flowchart for the reload evaluation process. The main product of the analysis is the reload safety evaluation (RSE) report and the updates to the core operating limits report (COLR). The figure qualitatively provides the depth and breadth of these analyses. As an example of COLR, Arkansas Nuclear One Unit 1 (ANO-1) set a list of core operating limits for cycle 25 [29]:

- Variable low reactor coolant system (RCS) pressure – temperature protective limits
- Shutdown margin (SDM)
- Physics tests exceptions – mode 1
- Physics test exceptions – mode 2
- Regulating rod insertion limits
- Axial power shaping rods (APSR) insertion limits

2. FRAMATOME.

- Axial power imbalance operating limits
- Quadrant power tilt (QPT)
- Power peaking
- Reactor protection system (RPS) instrumentation
- RCS pressure, temperature, and flow departure of nucleate boiling rate (DNBR) limits
- RCS loops – modes 1 and 2
- Boron concentration.

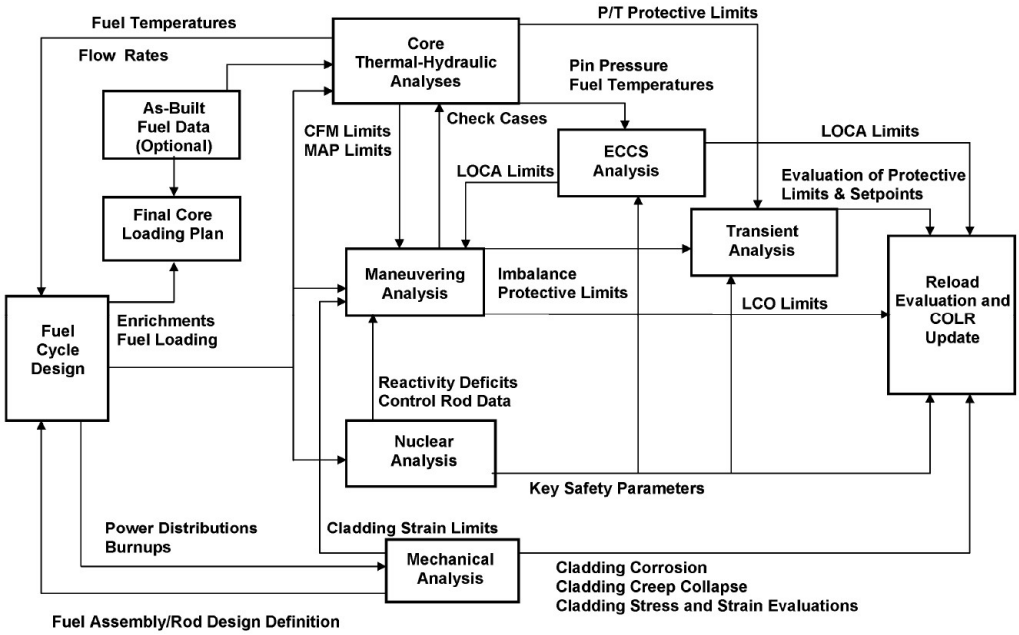

Figure 4-1. AREVA fuel reload evaluation flow chart [28].

Figure 4-2 shows the linear heat rate limit expressed 'kW/ft' as a function of assembly burnup from the analysis of the LOCA event of the ANO-1 cycle 25 [29]. The same reference provides DNBR power peaking factor limits that were designed to protect the initial conditions assumed in the DNBR loss flow transient analysis. Other limits are provided in the same reference. It is quite apparent that safety analyses and core design are coupled within the methods.

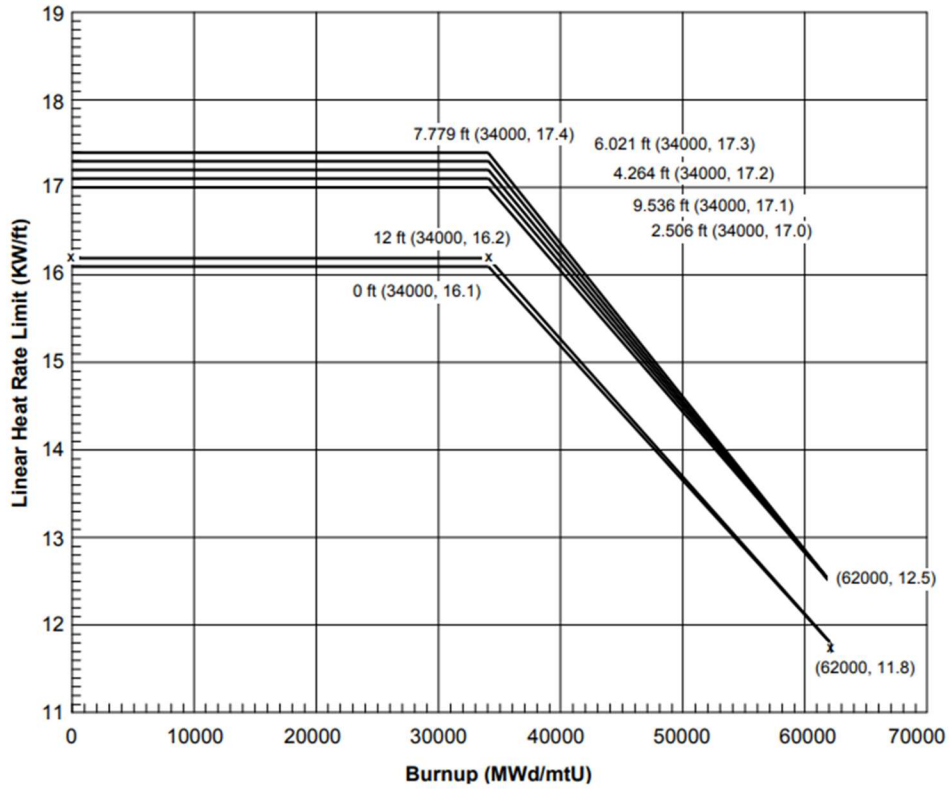

Figure 4-2. LOCA linear heat rate limit of Mark-B-HTP fuel of ANO-1 cycle 25 [29].

The WCAP-9273-NP-A [30] is the non-proprietary report that describes the Westinghouse RSE methodology. The method for RSE is based on the concept of 'bounding analysis.' The analysis assumes the existence of a reference analysis and on a reload-basis, key safety parameters for the reload core assume values that are conservatively bounded by those used in the reference analysis. If all the parameters are bounded, the reference safety analysis holds. If a parameter violates those bounds, further analysis is deemed necessary. The process of comparing the reload parameters to the reference parameters is also called reload safety analysis checklist (RSAC).

An important aspect that must be considered in the reload is the impact of the method by which the reactor is controlled to ensure that peaking factors experienced during the operation of the core remains within the limits assumed in the plant safety analysis. With the exception of the few plants for which a continuous monitoring of 3-D core power distribution is employed, most monitoring is performed with periodic surveillance as required by the technical specifications. There are two peaking factors of interest. The first is the heat flux hot channel factor, F_Q, defined as the ratio between the maximum linear heat rate and core average linear hear rate. The second, $F_{\Delta H}$, is sometimes called the assembly enthalpy rise, which is the ratio between assembly power and core-averaged assembly power.

Core power distributions to be considered in the safety analyses are characterized by defining peaking factors and axial power shapes. Two non-proprietary reports—WCAP-8403 [31] and WCAP-17661-NP, Revision 1 [32]—described the methodologies by which the reactor is controlled to operate within the safety limits. These are known as constant axial offset control (CAOC) and relaxed axial offset control (RAOC). These two procedures were developed by Westinghouse and are currently widely adopted by plant operators.

Power shapes need to satisfy the criteria of licensability and operability as follows:

- Licensability: The analyses need to show adequate safety margin limits, even when peaking factors and axial power shapes are pushed to technical specification limits.
- Operability: Control and set points associated with the assumed power shape need to ensure operability (e.g., to prevent spurious reactor trips).

Several parameters affect the core axial distributions, such as control rod insertion (e.g., full-length and part-length), burnup history, power level, and xenon distribution. Therefore, a real core design must include a long suite of operational scenarios that exercise these variations, which are not limited to base load constant power operation. For a given core design, the analysis may result in thousands of individual power shapes representing a range of power levels, xenon shapes, and control rod positions. The analysis must also be performed at different cycle times (e.g., core average burnups).

The Dominion Energy reload analysis methodology (2003-vintage) shows the COLR and RSAC were originally based on the Westinghouse methodology for the safety analyses [33]. The core design here is instead performed with the Studsvik core management system (e.g., CASMO-4 and SIMULATE-3).

4.2 Method for Technology-Neutral Cycle Reload Analysis

The objective of this project is to develop a methodology—or at least a framework—for a technology-neutral or fuel-product-independent core reload design optimization methodology. However, to entice utilities to enable its consideration and implementation, a strategy must be devised to minimize the impact to their licensing basis. Unless regulatory risks are minimized or eliminated, utilities will not be keen to change the status quo, established methods, and existing processes. In addition, it must be recognized that core reload safety analysis are established and rather complex processes often requiring proprietary data, methods, and procedures exist.

The proposed technology-neutral method should comply as much as practical with the interfaces currently in place to minimize utility and fuel vendor impacts. The vision is to assemble a plug-and-play architecture that will enable a utility to independently enter data on its own and align well with established processes and constraints. The solution should be a sort of applied programming interface (API) that will ease entering a minimum set of data with minimum effort, then execute the algorithm to achieve an optimized core design for the reload design that can be benchmarked with established core design practices. The degree by which the new method is folded into the licensing basis will be up to the utility and based on a cost-benefit analysis and other technical or commercial constraints.

The interface should incorporate the dependency with the safety analysis is a critical step in the process. The following is a possible strategy on the interfaces when dealing with Chapter 15 of FSAR. The set of scenarios are divided between the non-LOCA and LOCA events in the following sections.

4.2.1 Non-LOCA Events

For the non-LOCA methodology, a conservative/bounding approach is suggested to minimize impact on the existing methods in place. The boundedness of the assumptions can be confirmed with a series of plant-specific sensitivity studies. Those sensitivity studies can be part of future submittals to the NRC if a utility desires to pursue updating the licensing basis evaluation model. Confining the methodology to be plant-specific will narrow the scope to justify the applicability of the methodology and ease the licensing with a very focused safety evaluation report (SER).

A reload safety analysis confirmation process, or RSAC-equivalent, should be an integral part of the optimization algorithm considered for the fuel reload. For Westinghouse-served plants, this process would either replace or need to complement the RSAC checklist, WCAP-9272. This new ‘RSAC’ should be designed to confirm bounding assumptions and set points assumed in the analysis. Ideally, the process should be fully automated with automatic tracking of violation and automatic analysis parameter adjustments to meet the criteria.

Quality attributes of the methodology being proposed should include the following:

- The methodology references can be incorporated or align well with the technical specification list of references.
- Sensitivity studies must be performed to determine the most conservative plant conditions.
- SER may list specific limits dictated by limitation in the assessment or bounding assumptions in the methodology. This SER limitations should be considered in the analysis.
- Uncertainty allowances applied in initial conditions and reactivity parameters must be consistent with current practices, such as the moderator temperature coefficient (MTC).
- The calculated radial peaking factor, used for the hot rod calculations for DNBR analysis, should be normalized to the technical specification or COLR value to ensure all times in life are covered.
- A conservative void model may be selected for all reactivity feedback calculations.
- Subchannel code dynamic gap conductance model for the hot rod should be calibrated to conservative, bounding fuel average temperatures.
- The boron concentration should be adjusted (or increased) such that the initial hot full power (HFP)-Unrodded Xenon-free MTC reaches the technical specification limit to ensure all conditions over the cycle are bounded.
- For the end of cycle (EOC) calculations, the critical boron plus some margin could be taken.
- The DNBR calculation should be performed with a conservative radial power distribution with the peak rod power set to the technical specification or COLR limit to ensure the power distribution bounds the entire cycle.
- The updated methodology should be performed for both the positive and negative limit of the axial flux difference (AFD) operating band at HFP to determine the most limiting case.

A list of possible RSAC parameters for the non-LOCA can be:

- Moderator feedback coefficient
- Doppler feedback coefficient
- Delayed neutron fraction
- Radial and axial peaking factors (power distributions)
- AFD operating band
- Trip reactivity worth.

A dialogue with the utility will be necessary to define the comprehensive list of parameters to be considered. A demonstration analysis could assume a set of parameters that could be easily extended by the utility on their own.

4.2.2 LOCA Events

The LOCA break spectrum is typically divided in two segments. The first set is for the traditional LBLOCA (e.g., double-ended guillotine break or split break), while the second searches for the limiting small break (SB) LOCA (SBLOCA). The second set often performed following a deterministic approach to ease licensing, albeit examples of licensed BEPU methods are available [35]. The LBLOCA BEPU methodology showed that better management can control the operation margin [36].

The interface parameters are most likely similar to the current process (i.e., RSAC). However, the new methodology may allow a more realistic representation of the actual plant/core state point. For

instance, there is no need to pass specific fuel performance data, such as pellet average temperature (TFUEL) or rod internal pressure (RIP) during the LOCA analysis. Thermo-mechanical tools, such as TRANSURANUS, can be used to compute those physics.

The LOCA analysis extracts data from the core design database and builds a system response database, which then feeds a full core (e.g., assembly-by-assembly or even pin-by-pin) thermo-mechanical response simulation. In this case, the list of parameters for the reload confirmation can be reduced dramatically when compared to the current practice. The reason is that most parameter flow-down occurs naturally from the core design rather than building layers of assumptions that need to be verified in the typical segregated process.

For example, the list for LOCA could be limited to:

- Fuel features and composition consistent with the core design
- Maximum enthalpy rise peaking factor ($F_{\Delta H}$)
- Maximum relative power in hot assembly (P_{HA})
- Maximum K(z) curve and F_Q or maximum linear heat rate (LHR)
- Axial offset at 100% power
- Core axial power shape model
- K_{eff} for post-LOCA long-term core cooling (e.g., all rods out, no xenon, most reactive time in core life, etc.)
- Maximum subcritical boron concentration
- K_{eff} for post-LOCA short-term subcriticality minimum accumulator boron concentration
- Minimum accumulator boron concentration
- Maximum RCS boron concentration
- Sump boron dilution at hot leg switchover
- Return to licensed core power (LCP)
- Minimum control rod worth
- LCP
- Maximum full power MTC.

4.2.3 Areas for further Investigation

There are also areas of further investigation that remain:

- The non-LOCA analysis presented in Section 4.2.1 focused on the loss of flow or locked rotor scenario for non-LOCA. As other events are reviewed, the list of parameters may be extended
- For the LOCA events, attention should also be paid to the long-term cooling (LTC) aspect, which has some peculiarity in analysis space
- Also, ancillary analyses such as grid crush must be considered
- Need to assess impact of LOCA forces (e.g., probably linked to the bullet above)
- Need a position for containment analysis or at least its interface to the analysis of the LOCA events.

4.3 Risk-Informed Methodology

Power plant operators are looking for a much broader spectrum of operation modes of their plants as they seek improving the economics. There is an opportunity to consider a risk-informed approach when performing safety analyses to support the introduction of ATF products and drive a higher fuel utilization with higher burnup and higher enrichment (e.g., LEU+ and HALEU).

Another driver is the consideration by some utilities, especially in the deregulated market, for more flexible operation that may include load follow, or in general, deviation from the traditional base load operation mode that characterized the U.S. NPP fleet so far. Flexible, load follow operation is common in other markets, most relevantly in France.

Finally, utilities may look at ways to commoditize the fuel supply. Especially in United States, fuel type transition costs are a high barrier justifying multi-cycle, long duration contract between utilities and fuel suppliers—in most cases, decades long. Changing fuel product requires analyzing the core in a 'fuel transition' pattern that adds complexities. Note that NPPs in other countries are in a constant 'fuel transition' situation. The analysis of mixed cores requires fuel-technology-neutral evaluation models. On the contrary, established methods are often developed and licensed by the fuel vendors and are tailored to their specific fuel product. A utility could be interested in having the capability of routinely analyzing mixed cores. The mix can be a combination of different fuel product in different regions of the core and the adoption of ATF assemblies together with older assemblies, etc. All these drivers point to the need of generic technology-neutral methods to perform the reload safety analyses.

Significant work has been done to develop risk-informed performance-based (RIPB) approaches, especially for the deployment of the advanced reactors. The U.S. nuclear regulatory commission has been seeking a generic licensing framework that is intended to be risk-informed and technology-neutral. The outcome is the new drafted rule 10 CFR Part 53, an outcome of the nuclear energy innovation and modernization act (NEIMA) which was signed to law in 2019. This risk-informed and performance-based licensing framework paves the way for regulatory reviews to be aligned with the inherent safety characteristics, smaller reactor cores and simplified designs of advanced reactors. Over the last several years, the industry's licensing modernization project developed a roadmap, NEI 18-04 [37], which is intended to guide reactor designers and developers in the new regulatory framework.

In a RIPB framework, decision on the acceptability of a design or design change are based on frequency-consequence targets such as those display in Figure 4-3.

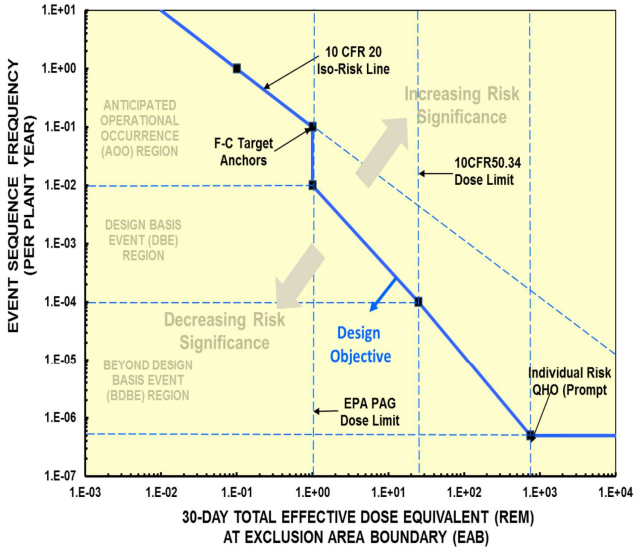

Figure 4-3. Frequency-Consequence Target [37].

The RIPB approach can play an important role to address some of the issues outlined above. Note that the new rule is not expected to become the law until 2025. However, even if the current rules are framed for a more deterministic approach, some degree of risk-informed analysis could add insights on solutions which otherwise would not being considered.

The implementation of RIPB approaches for reload analyses has been one of the objectives of this project. However, a two-staged approach is recommended to facilitate the deployment of new methods in the industry. Section 4.3.1 summarizes the pros and cons of a full PRA-driven RIPB approach. Considering some of the challenges, especially from a licensability standpoint, a pragmatic near-term approach is suggested in Section 4.3.2 and recommended for this project.

4.3.1 Prospect for Risk-Informed Approach

Even if the current rules are based on deterministic approaches, RIPB analyses could add insights to solutions that would otherwise not be considered.

The 10 CFR Part 53 rule is currently expected to be issued as final rule by July 2025 [38]. The draft rule is still subject to public comments. The industry expressed concerns that the implementation of the rule could be cumbersome and run against a more streamline process, the original intent of the NEIMA. Traditionally PRA has been used to provide risk insights but never folded in the design process itself. For the operating fleet, PRA has been used for on-line risk maintenance, to define mitigating system performance index (MSPI) (10 CFR 50.65), plant modifications risk impacts, risk reduction initiatives, significant determination process for NRC violations, risk significant insights, license amendment requests (LAR), outage schedule review, inspection and audit support (importance measure), etc. The adoption of a risk-informed reload design would be a new and challenging application from a regulatory standpoint.

PRA involves the evaluation of a large spectrum of scenarios, a much wider spectrum than the set of scenarios considered for the safety analyses in standard review plan (SRP) Chapter 15. In most cases, these determinations are based on rather simple simulation of the plant response to initiating events. These analyses are often called ‘success criteria’. In PRA Level-1, the objective is to simply determine the core damage frequency where the answer sought is a binary pass or fail. Regulatory limits govern the criteria for the failure and act as surrogate safety limits (e.g., PCT) for determining failures with little relationship to the actual system performance.

Advancements in modeling and simulation and computational performances provide the opportunity to challenge this ‘status-quo’ and hold the promise for the PRA to provide more insights on the actual safety margin. At the early stage of the research, it was recognized that a plant ‘super-model’ could be built to cover a more complete spectrum scenarios which includes both events considered for Chapter 15 safety analyses as well as events progression that must be analyzed for PRA success criteria; therefore, replacing simplistic ROM such as MAAP (modular accident analysis program) or CONTAIN (computer code for nuclear reactor containment analysis) computational tools. This initial goal has been partially demonstrated with the work performed so far under this project.

However, moving forward, current regulatory framework and established industry practices must be considered in what is here called a pragmatic approach to risk-informing plant reload analyses. This will permit a near-term go-to-market strategy while rulemaking proceeds to allow a fully RIPB licensing process. This pragmatic or graded approach is described in the next section.

4.3.2 Programmatic Approach to Risk-Informed Methodology

It is worth noting that 10 CFR 50.46 specifically calls out UO_2 and Zircaloy-based cladding in the regulation. In order to extend this regulation to other cladding types, such as those being proposed for use in ATF, rulemaking will need to occur to remove these specificities. The 10 CFR 50.46 acceptance criteria were developed as ‘surrogate’ to fuel failure mechanisms and have been successfully applied so

far to ensure the safety of the power plant operation from cycle to cycle. Ultimately, the rule is ensuring that: (1) a core coolable geometry is maintained; (2) radioactivity release due to core damage is prevented; and (3) hydrogen generation and subsequent detonation (e.g., catastrophic failure) does not occur.

Established evaluation models were developed to align well with the SRP, such as NUREG-0800. The SRP is not a rule, but the framework by which regulators are expected to review and accept license amendment applications. The SRP was designed around existing LWR technology and traditional UO2 and Zircaloy-based cladding fuel. However, the applicability of current SRP to advanced LWR technologies and advanced fuels is still under investigation.

The SRP also sets specific acceptance criteria for events depending on their classification in anticipated operational occurrences or DBAs. An aggressive risk-informed alternative to these analyses would be to consider the frequency of each licensing basis event, which would be derived from PRA models. We are instead proposing here a methodology that preserves the intent of the SRP and offers a graded approach that maintains layers of conservativism (i.e., deterministic approach and defense-in-depth). The RIPB aspects are included in regard to the choice of acceptance criteria (or performance criteria) and metrics used to assess the response of events in relation to the selected acceptance criteria.

In general, a set of goals and constraints are identified for the development of the methodology:

- Consider performance-based acceptance criteria and metrics for the safety analysis that are similar or consistent with the current ones to minimize licensing risks/efforts.
- Remove unnecessary layers of conservatisms across the physics-based modeling by resolving dependencies and uncertainties in a realistic fashion.
- Consider an integrated evaluation model for both safety analyses (e.g., Chapter 15 analyses) and core reload design and safety analysis, which truly represents the state of the plant at a given point in time. The framework should easily allow the confirmation of the safety analyses at the reload-basis rather than generic conservative safety analysis limits applicable to multiple cycles.
- Consider regulatory implications and ensure that the eventual adoption by the industry is viable and does not introduce additional regulatory burden.

The third goal above is specifically relevant when considering the previously discussed much wider operation mode spectrums considered by the utilities. That trend would make it very difficult to define ‘a-priori’ the bounding plant state to consider in the analysis. A stretch goal is to yield an extension of the online core monitoring system that not only considers the typical COLR set points, but also includes/integrates the safety analysis limits if the economics of the operation justify. This goal also would consider realistic (e.g., transient) core peaking factors during the cycle, for example, which account of the operation history and optimize operational flexibility moving forward.

The methodology considered so far in this project was limited to a base load operation mode assumption. The analysis needs to be extended beyond base load operation to consider effects of Xenon transients to axial power shapes (see the CAOC/RAOC methodologies discussed previously).

A simple demonstration of a methodology that would consider load follow maneuvering can be built following the approach presented in [31], which was used to obtain the results presented in Figure 4-4, Figure 4-5, and Figure 4-6. In fact, Figure 4-6 provides examples of ‘flyspecks’ calculated for various accidents (e.g., non-LOCA)—from non-proprietary WCAP-8403 [31]—for various 3- and 4-loop boration or dilution malfunction events. Note that the achievable peaking factors should be a function of burnup. This is an area to consider in the methodology since it could uncover margin.

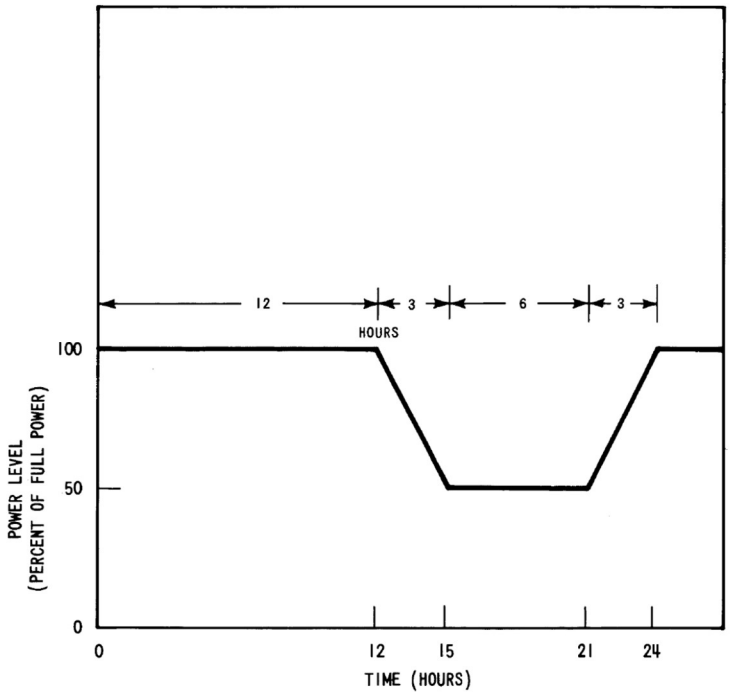

Figure 4-4. Typical load follow cycle [31].

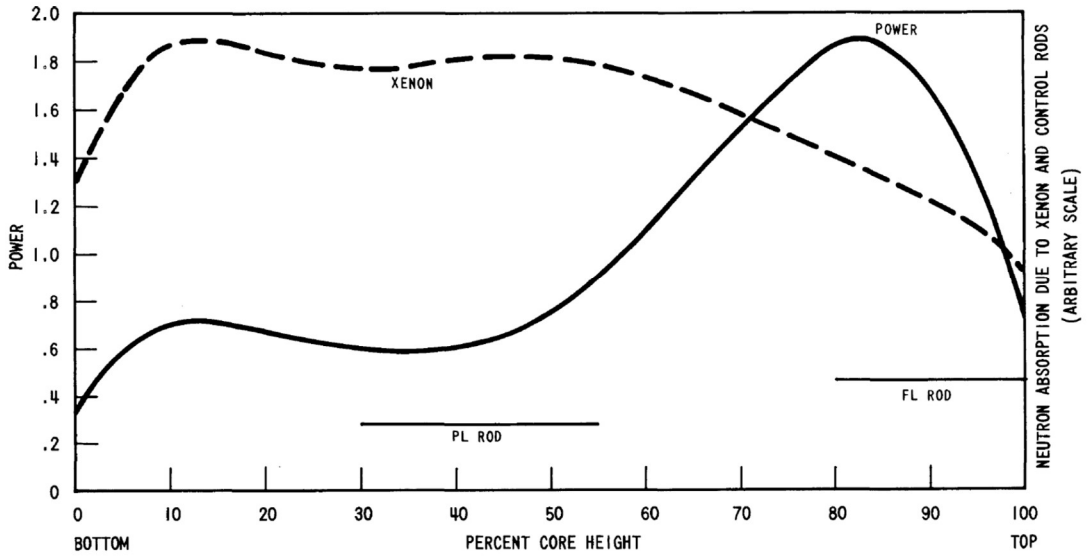

Figure 4-5. Xenon-induced power swing [31].

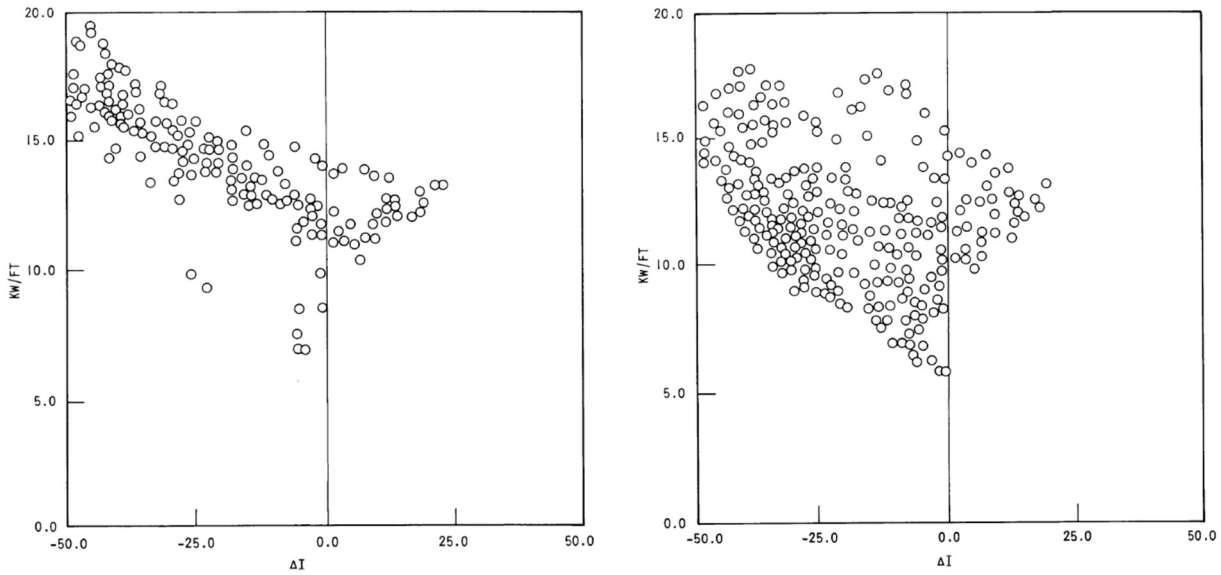

Figure 4-6. Example of flyspecks in a 3-loop plant (left: boration/dilution malfunction or operator error flyspeck; right: plant control bank malfunction flyspeck) [31].

A partnership with a utility at this stage of the project would be beneficial to identify the areas of interest and steer the subsequent developments. The collaboration could begin by identifying a list of quality attributes, brainstormed scenarios, and requirements to focus the framework development in order to maximize its value proposition to the industry.

With regard to the goal of considering performance-based acceptance criteria and metrics for the safety analysis, it is worth noting that 10 CFR 50.46 limits, such as the PCT, maximum local oxidation (MLO), and core-wide oxidation (CWO), are surrogates to ensure the cladding integrity and prevention of catastrophic failures, as well as to limit the amount of hydrogen that could lead to a containment catastrophic failure.

However, the validity of these surrogates when considering more advanced fuel is questionable. Actual fuel failure mechanisms should be used as the basis for established acceptance criteria instead of regulatory 'surrogates'. This will allow more realistic assessments of the consequences of a postulated event. The computation of the dose or radiological impact is still beyond the scope of the analysis. However, acceptance criteria, e.g., design-specific source terms, that can better describe failure mechanisms and resulting consequences are desired and attainable within the scope of the project.

Consistent propagation of uncertainties across plant parameters and physics can yield a more coherent BEPU approach. The limit deviation from the established method of the principles proposed in Section 4.2 should be considered in the methodology development.

The LWRS/RISA pathway GA-based plant reload optimization framework is currently under development for the demonstrative methodology. The choice of tools (e.g., CASMO/SIMULATE, RELAP5-3D, TRANSURANUS) are not 'required' tools. The framework is developed to enable the applicant to consider tools of their choice.

The multi-physics approach to problem resolution, as illustrated in Figure 4-7, is also a potential solution to the goals of the project. The level of coupling (e.g., strongly, weakly, one-way, two-way, explicit, implicit, etc.) between the physics tools is a trade-off between convenience and potential margin uncovered by the coupling.

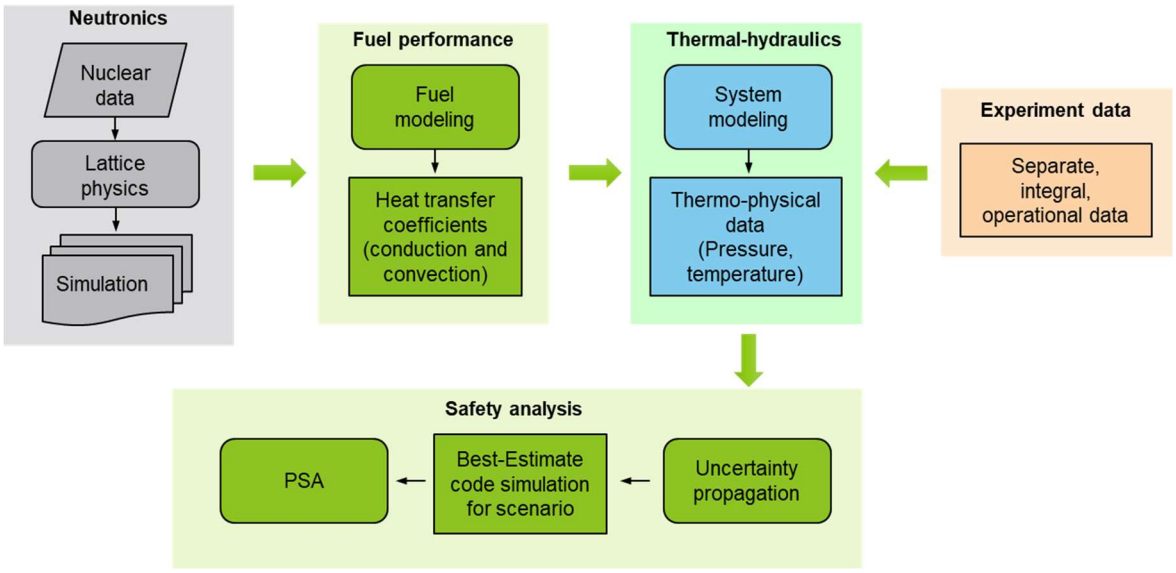

Figure 4-7. A framework to enable a multi-physics approach.

4.4 Remarks and Needs

The currently developing GA-based Plant Reload Optimization Project framework is more focused on PWR technology rather than BWR, in which the models are available and the general framework more mature.

In order to demonstrate the value of the proposed solution, a few key questions must be addressed:

- How much margin is locked in not re-evaluating the safety analyses coupled with core design?
- How much margin in the proposed optimization algorithm can be exposed and in which form? Is there a reduction in the number of feeds? Is there an extension of cycle length?
- How much margin is locked in the current regulatory limits (e.g., 10 CFR 50.46 or AOO criteria) versus technology-specific performance?

A dialogue with a utility may uncover higher priority questions. This assessment is currently limited to an opinion that must be validated. To answer these questions, the following milestones must be achieved:

- Complete the optimization algorithm, including the ability to perform multi-objective optimization.
- Complete an end-to-end core design that is limited to the equilibrium core but includes 'real-life' aspects, such as CAOC/RAOC consideration. This core design can form the baseline.
- Ensure consistency between the safety analysis and the core design. In other words, mimic the RSAC process to some extent.
- Identify the constraints and objectives for the optimization.
- Identify the list of 'risk-informed' items to explore in the analysis space.

Once these key milestones are achieved, the analysis can proceed by quantifying the margin opportunity and its associated economic benefits to answer the key questions listed above.

5. BENCHMARK STUDY ON CORE DESIGN AND FUEL PERFORMANCE TOOL

A benchmark study was conducted for an evaluation of available reactor core design and fuel performance computer codes to determine tool capability and applicability for the fuel reload optimization framework. The framework has three different areas of design: (1) core design; (2) fuel performance; and (3) system analysis. The RELAP5-3D code was selected as the best estimate system analysis code. It is fully validated and versatile to be tightly coupled with RAVEN, which is the main operating tool for the optimization framework. For the core design and fuel performance, different codes are considered from newer high-fidelity tools to more established software currently used by the nuclear industry. Three different core design codes—SIMULATE, PARCS, and VERA-CS—and two different fuel performance codes—TRANSURANUS and BISON—were assessed. The SIMULATE and TRANURANUS codes ultimately were selected based on the needs of the GA-based optimization framework. Figure 5-1 shows a schematic diagram of the plant reload optimization framework.

Details of the benchmark study are provided in Appendix A.

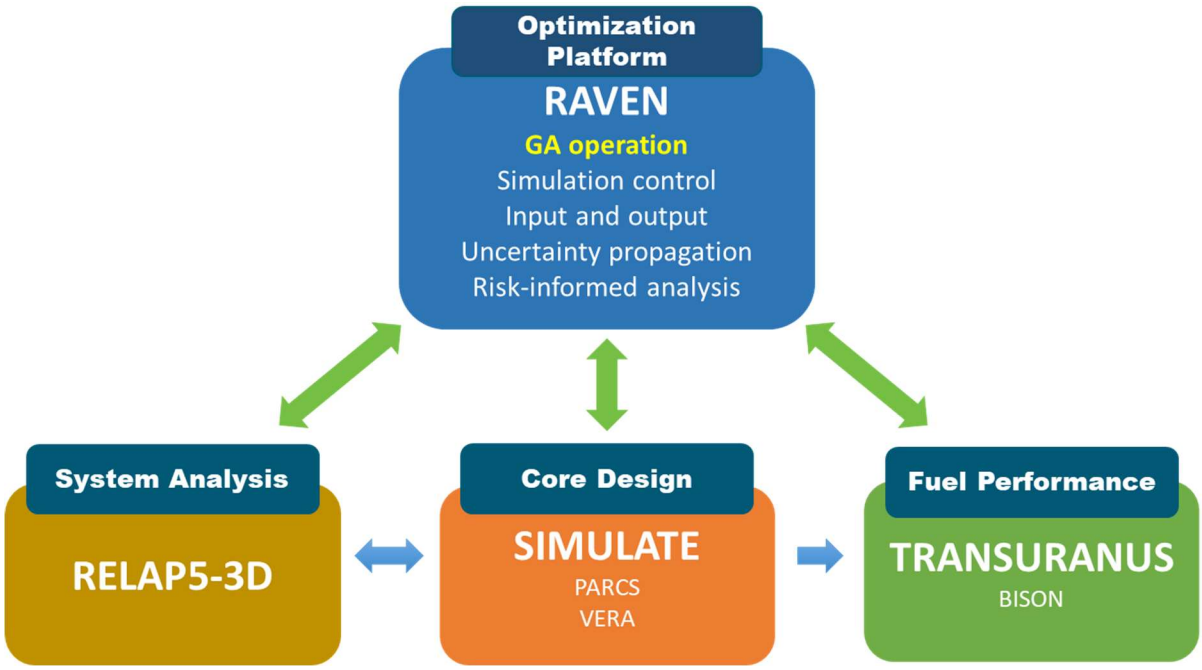

Figure 5-1. Schematic diagram of plant fuel reload optimization framework.

6. REFERENCES

[1] Choi, Y.-J., et al., "Demonstration of the Plant Fuel Reload Process Optimization for an Operating PWR," INL/EXT-21-64549, Idaho National Laboratory, 2021.

[2] Andersen, B. D., "A Machine-Learning Based Approach to Minimize Crud Induced Effects in Pressurized Water Reactors," Dissertation, North Carolina State University, 2021.

[3] Castillo, A., C. M. del Campo, J.-L. Montes-Tadeo, and J. L. François, "Comparison of heuristic optimization techniques for the enrichment and gadolinia distribution in BWR fuel lattices and decision analysis," *Annals of Nuclear Energy*, Vol. 63, pp. 556-564, 2014.

[4] Andersen, B., G. Delipei, D. Kropaczek, and J. Hou, "MOF: A modular framework for rapid application of optimization methodologies to general engineering design problems," arXiv preprint arXiv:2204.00141, 2022.

[5] Alfonsi, A., C. Rabiti, D. Mandelli, J. Cogliati, C. Wang, P. W. Talbot, D. P. Maljovec, and C. Smith, "RAVEN Theory Manual," INL/EXT-16-38178, Rev. 4, Idaho National Laboratory, Idaho Falls, ID, USA, 2021.

[6] The RELAP5-3D© Code Development Team, "The RELAP5-3D© Code Manual Volume I – V Rev 4.4", Idaho National Laboratory, 2018. (Publicly not available)

[7] Alfonsi, A., et al., "RISA Plant Reload Process Optimization: Development of design basis accident methods for plant reload license optimization", INL/EXT-20-59614, Idaho National Laboratory, 2020.

[8] Holland, J. H., "Genetic Algorithms", Scientific American, Vol. 267.1, pp. 66-73, 1992.

[9] Zeng, K., Stauff, N. E., Hou, J., and Kim, T. K., "Development of Multi-Objective Core Optimization Framework and Application to Sodium-Cooled Fast Test Reactors", Progress in Nuclear Energy, Vol. 120, 2020.

[10] Michalewicz, Z., "Genetic Algorithms. + Data Structures. = Evolution Programs", Third, Revised and Extended Edition, Springer, 1996.

[11] Bingham D., "Virtual Library of Simulation Experiment: Test Functions and Datasets of Optimization Test Problems", https://www.sfu.ca/~ssurjano/optimization.html, Retrieved August 18, 2022.

[12] Mishra, S, "Some New Test Functions for Global Optimization and Performance of Repulsive Particle Swarm Method", Munich Personal RePEc Archive, 2007

[13] Simionescu, P.A., "Computer Aided Graphing and Simulation Tools for AutoCAD Users (1st ed.)", Boca Raton, FL: CRC Press., ISBN 978-1-4822-5290-3, 2014.

[14] Townsend, A. "Constrained optimization in Chebfun", http://www.chebfun.org/examples/opt/ConstrainedOptimization.html, Retrieved August 18, 2022.

[15] Silvano, M., and Toth, P., "Knapsack Problems: Algorithms and Computer Implementations", John Wiley & Sons, Inc., 1990.

[16] Deb, K., Pratap, A., Agarwal, S., and Meyarivan, T., "A Fast and Elitist Multiobjective Genetic Algorithm: NSGA-II", IEEE Transactions on Evolutionary Computation, Vol. 6, No'. 2, pp. 182-197, 2002.

[17] Smith K.S., Umbarger J. A., VerPlanck D. M., SIMULATE-3: Advanced three-dimensional two-group reactor analysis code user's manual, Studsvik Scandpower, Studsvik/SOA-95/15 Rev 2, 1995.

[18] TRANSURANUS HANDBOOK, V1M2J19, 2019

[19] Erbacher, F., and S. Leistikow, "Zircaloy Fuel Cladding Behavior in a Loss-of-Coolant Accident: A Review," in Adamson, R., and L. S. Van (eds.), *Zirconium in the Nuclear Industry*, ASTM International, West Conshohocken, PA, USA, 451–488, 1987.

[20] Parisi, C., and Y.-J. Choi, "Risk-Informed Multi-Physics Best-Estimate Plus Uncertainties (BEPU) Application Development of RELAP5-3D Perturbation Model," INL/EXT-20-59594, Idaho National Laboratory, 2020.

[21] So. E, Parisi, C., and Choi, Y.-J., "Risk-Informed Multi-Physics Best-Estimate Plus Uncertainties (BEPU): Demonstration of LOCA Scenario-Based Reflood Phenomena," INL/EXT-21-644450, Idaho National Laboratory, 2021.

[22] NRC, FLECHT SEASET Program Final Report, NUREG/CR-4167, 1985

[23] Ihle, P., and K. Rust, "FEBA-Flooding Experiments with Blocked Arrays Evaluation Report," Kernforschungszentrum Karlsruhe, KfK 3657, 1984.

[24] Andersen, J. M. G., K. H. Chu, and J. C. Shaug, "BWR Refill-Reflood Program, Task 4.7—Model Development, Basic Models for the BWR Version of TRAC," NUREG/CR-2573, EPRI NP-2375, GEAP-22051, 1983.

[25] Ishii, M., "One-dimensional Drift-flux Model and Constitutive Equations for Relative Motion Between Phases in Various Two-phase Flow Regimes," ANL-77-47, Argonne National Laboratory, Argonne, IL, USA, 1977.

[26] J. H. Park, and Y. H. Jeong, "Modeling of droplet diameter changes during reflood into RELAP5/Mod3.3," *Nuclear Engineering and Design*, Vol. 393, Art. 111791, 2022.

[27] Hochreiter L.E., et al., "Dispersed flow heat transfer under reflood conditions in a 49 rod bundle: test plan and design – results from tasks 1–10", USNRC/ PSU ME/NE-NRC-04-98-041 Report 1, Revision 1, 2001

[28] AREVA NP Inc., "Safety Criteria and Methodology for Acceptable Cycle Reload Analyses," Revision 9, BAW-10179NP, Paris, France, 2016.

[29] U.S. Nuclear Regulatory Commission, "Arkansas Nuclear One, Unit 1 Cycle 25 Core Operating Limits Report," ML13172A083, Washington, D.C., USA, 2013.

[30] Westinghouse Electric Corp., "Westinghouse Reload Safety Evaluation Methodology," WCAP-9273-NP-A, Pittsburgh, PA, USA, 1978.

[31] Westinghouse Electric Corp., "Topical Report: Power Distribution Control and Load Following Procedures," WCAP-8403, Pittsburgh, PA, USA, 1974. Available at: https://www.osti.gov/servlets/purl/4242391 (accessed 11 August 2022).

[32] Westinghouse Electric Corp., "Improved RAOC and CAOC FQ Surveillance Technical Specification," WCAP-17661-NP, Pittsburgh, PA, USA, 2013.

[33] Dominion Energy, "Virginia Electric and Power Company's (Dominion) Core Operating Limits Report, (COLR) for Surry Unit 2 Cycle 19 Pattern AM, Revision 0. In Attachment 2: VEP-FRD-42 Rev. 2.1-A, 'Reload Nuclear Design Methodology,'" Richmond, VA, USA, 2003.

[34] Westinghouse Electric Corp., "FULL SPECTRUM™ LOCA Methodology," Pittsburgh, PA, USA, 2014. Available at: https://westinghousenuclear.com/Portals/0/Flysheets/NS-ES-0209%20FSLOCA_PWR.pdf (accessed August 11 2022).

[35] Frepoli, C., "An Overview of Westinghouse Realistic Large Break LOCA Evaluation Model," *Science and Technology of Nuclear Installations*, Vol. 2008, Art. 498737, 2008.

[36] R. O'Dell, P. Martin and D. Larry, "Development Considerations of AREVA NP Inc.'s Realistic LBLOCA Analysis Methodology", 2007.

[37] Nuclear Energy Institute, "Risk-Informed Performance-Based Technology Inclusive Guidance for Non-Light Water Reactor Licensing Basis Development", NEI 18-04 Revision 1, August 2019

[38] U.S. Nuclear Regulatory Commission, "Part 53 – Risk Informed, Technology-Inclusive Regulatory Framework for Advanced Reactors", Available: https://www.nrc.gov/reactors/new-reactors/advanced/rulemaking-and-guidance/part-53.html.

[39] OECD Nuclear Energy Agency, "Review of Nuclear Fuel Experimental Data - Fuel Behaviour Data Available from IFE/OECD Halden Project for Development and Validation of Computer Codes", 1995.

Appendix A – Benchmarks of Core Design and Fuel Performance Tools

This appendix provides a summary of available tools that could be used by utilities within the proposed framework which would offer a flexibility to employ already-approved fuel performance evaluation tools, which should reduce efforts for regulatory approvals. More specifically, the objective of the study presented in this Appendix is the assessment of features and modeling capabilities of various software tools available within the industry to determine their applicability to the plant reload optimization framework and their capabilities to meet the postulated requirements.

A-1. Core Design Tools: VERA-CS, SIMULATE-3, and PARCS

Three core design tools, VERA-CS, SIMULATE and PARCS, were used for the benchmark. The parameters of interest investigated include the simulation time capability, computational efficiency, integration with upstream cross-section generation modules, user friendliness, and ATF applicability.

The controlled benchmark calculations for this purpose are the three exercises in the TVA Watts Bar Unit 1 (WB1) Multi-Physics Benchmark with a focus on two main simulations: stand-alone 3-D neutronics model at hot zero power (HZP) conditions and multi-physics steady-state model for hot full power (HFP) conditions at the beginning of cycle (BOC). This allows for the comparison of code capabilities with details originating from a real-world problem. The use of this benchmark is to identify optimal code capabilities by performing different multi-scale calculations from the pin cell up to full core HZP and HFP operating conditions.

A-1.1 Description of Reactor Core Simulation Codes

Throughout history, for the steady-state and transient core analyses, the industry and U.S. Nuclear Regulatory Commission (NRC) standard has been the use of conventional fidelity codes which employ a two-step method. In the two-step method, a series of lattice physics calculations are performed as the first step to develop several sets of few-group homogenized cross-sections of each fuel assembly. These cross-sections are typically generated by solving a single fuel assembly with reflective boundary conditions using B1 leakage correction for different burnup and reactor conditions with various fuel temperatures, moderator densities, boron concentrations and control rod insertions. Following the generation of the few-group cross-sections, few-group nodal diffusion-based coupled neutronics/TH calculations are performed as the second step to calculate nodal flux, power, and core eigenvalues [2]. However, novel methods (one-step methods) for core analysis have been developed in recent years which include high fidelity advanced solvers and multiphysics coupling algorithms for explicit pin-by-pin transport solutions. The high fidelity is accomplished by integrating highly refined solvers for the coupled neutronics, TH, and thermo-mechanical phenomena. Some characteristics of these high-fidelity code suites include whole core neutron transport with the use of multigroup cross-section library directly without group condensation, ultra-fine mesh computational fluid dynamics/heat transfer solutions, and finite-element based thermo-mechanic solutions all obtained with explicit (fuel pin cell level) heterogeneous representations of the core.

Several differences exist between two-step and one-step methods. The one-step approach uses explicit pin-by-pin powers and burnup whereas the two-step approach uses pin power reconstruction-based diffusion solutions to approximate pin power and burnup distributions. Another difference is the node-averaged quantities calculated in the two-step approach in comparison to the pin local TH distributions in the one-step method. In comparison of the computational runtime, while the full set of lattice physics calculations for the two-step approach requires a significant amount of runtime, the full core evaluations are performed much faster as compared to the on-step approach computations. This indicates a significant

advantage of the two-step method over the one-step method for optimization and perturbation studies [A-1].

A-1.1.1 VERA-CS

The VERA simulation environment [A-2] was developed by the Consortium for Advance Simulation of Light Water Reactors (CASL) for the direct multi-physics coupling of existing high-fidelity physics code with capabilities for transient neutron transport, TH, fuel performance, and chemistry calculations and is optimized for spatial fidelity with an emphasis on performance and parallelization. The VERA-CS reactor simulation application includes the subset of these coupled physics codes needed for reactor core depletion over multiple cycles. The VERA-CS application in this work includes the direct neutronics transport code, MPACT [A-3], as well as the TH code, COBRA-TF (CTF) [A-4].

MPACT is a transient one-step code that has been applied to PWRs and BWRs. It relies primarily on the Method of Characteristics (MOC) coupled with a P3 transport with a fourth-order Legendre-based spatial flux expansion approach in a 2D/1D method for whole core transport. A multi-group approach is used where neutron cross-section data is taken from the SCALE 56-group ENDF-B/VII.1 library while accounting for subgroup resonance self-shielding. MPACT resolves the time-dependent two-group nodal diffusion equations using the coarse mesh finite difference (CMFD) method. An emphasis is placed on parallelization via spatial decomposition.

CTF is a TH simulation code designed for LWR core TH analyses. It employs a two-fluid/three-field modeling approach with both scalar and momentum subchannel discretization. It includes only limited internal conduction models for pin-level modeling; this leads to fidelity issues in the transient calculations, but the issues are negligible in the steady-state case.

A-1.1.2 SIMULATE-3

SIMULATE-3 is an advanced 3D two-group nodal code for analyses of both PWRs and BWRs. The code is based on the QPANDA neutronics model, which employs fourth-order polynomial representations of the intranodal flux distributions in both the fast and thermal groups and has been extensively benchmarked with measured data and higher order calculations [A-5]. This code can be used for fuel management, and core follow, as well as reload physics calculations. It can reconstruct the pin power distributions and perform multi-criteria searches on exposure, power, flow, etc. In addition, it can also generate D cross-sections and 1D/0D kinetics data for transient analyses. The code uses a simple heat balance model to calculate the enthalpy rise in specific nodes by assuming a number of factors. These factors include that the inlet flow and temperature distribution are known, the coolant flow is in parallel channels (e.g., no cross flow and the core outlet water remains subcooled), the heat is produced and deposited in the same node, and the pressure drop across the core is negligible (e.g., all water properties are evaluated at a single pressure) [A-6].

CASMO-4 computer code is used to generate nuclear data inputs for SIMULATE-3. It is a multi-group 2D fuel assembly burnup calculation program developed by Studsvik Scandpower intended for use on PWR and BWR pin cells or assemblies. CASMO-4 is a transport theory depletion code with its transport solution based on the MOC and an assumption of isotropic scattering. It models the true heterogeneous geometry of assemblies typical of today's LWR assemblies, including but not limited to gadolinium rods, burnable absorber rods, spacer grids, etc. This code can be run in partial-, full-, or multi-assembly geometry, and it produces two-group cross-sections that are homogenized for the input to SIMULATE-3 [A-7].

The cross-sections generated by CASMO-4 for the fuel assemblies and reflector are linked with SIMULATE-3 by another code known as CMS-LINK, which converts data provided by CASMO-4 into a tabular form presented in a binary library. The generated cross-sections are a function of different state points as defined in CASMO-4 and based on calculation of nodal-averaged cross-sections as a summation of 'partial cross-sections' [A-8].

The TH feedback parameters, such as fuel temperature are computed separately using a TH module known as the INTERPIN code [A-9], which computes the 3D fuel temperature by solving the 1D annular heat conduction equation for the average fuel pin of each node using the coolant temperature as a boundary condition. The code also allows for the use of pre-computed temperature tables and accounts for the physical changes (e.g., thermal expansion, irradiation-induced swelling of the fuel, fuel pellet cracking) with burnup by adjusting the conductivity of fuel and cladding.

A-1.1.3 PARCS

PARCS is the core neutronics code supported by the NRC and primarily used for modeling LWRs for steady-state, depletion, and transient calculations. PARCS solves the time-dependent two-group nodal diffusion equations using CMFD. Two different nodal solvers are available—the analytic nodal method (ANM) and the nodal expansion method (NEM). The pin power reconstruction capability can be used to provide pin-by-pin power information. Beyond diffusion problems, PARCS also includes an SP3 transport solver. PARCS can compute TH feedback using two different solvers. The first is called PATHS and consists of a four-equation drift flux model, while the second is a simplified 1D mass energy balance solver for PWR cores.

The POLARIS/PARCS computational suite uses POLARIS code [A-10] for lattice calculations to generate two-group macroscopic cross-sections parameterized for all potential core conditions (e.g., burnup, temperatures). The GenPMAXS converter provided with PARCS [A-11] is used to convert the POLARIS output format to the PMAXS format read by PARCS. PARCS uses these cross-sections to perform 3D core nodal diffusion calculations.

POLARIS is a 2D lattice physics code integrated into the SCALE [A-10] suite that is developed and maintained by ORNL. POLARIS is developed specifically for LWRs and uses a MOC transport solver together with the embedded self-shielding method (ESSM) to condense and homogenize the cross-sections. An effort was made to simplify the input deck as much as possible to allow the efficient development of lattice physics models for different LWRs. POLARIS is coupled with ORIGEN to perform depletion calculations and can be called by the SAMPLER stochastic tool within SCALE to sample cross-sections and manufacturing parameters.

In this core design tool benchmark study, POLARIS lattice calculations were performed using the SCALE 56-group ENDF/B-VII.1 cross-section library (a 252-group library also is available) to condense the cross-sections into two-groups and homogenize them in the whole assembly. These calculations are performed for different parametric points that cover the intended core conditions in PARCS.

POLARIS generates sets of parameterized macroscopic cross-sections for every fuel assembly in a LWR and for the reflector in the ‘t16’ format. This format cannot be used directly by PARCS for the core neutronics calculations. For this reason, the GenPMAXS code is used to convert the ‘t16’ files to PMAXS, which is the format read by PARCS. In general, GenPMAXS allows the conversion of cross-sections generated with various transport codes to PMAXS. Examples of additional codes are HELIOS, CASMO, and SERPENT.

A-1.2 Benchmark Specifications

A-1.2.1 Benchmark Description

The WBN1 is a Westinghouse four-loop PWR managed by the TVA that has been operating since 1996. It has a 3411 MWth power rating for the cycle in question (e.g., Cycle 1) with a 1.4% power upgrade in 2001, which raised the power rating to 3460 MWth. Figure A-1 shows a 2D slice of the WBN1 Cycle 1 full-core layout on the left with an axial layout of the fuel assembly on the right. The axial layout includes the upper and lower core plates, nozzles, gaps, Inconel, and Zircaloy spacer grids.

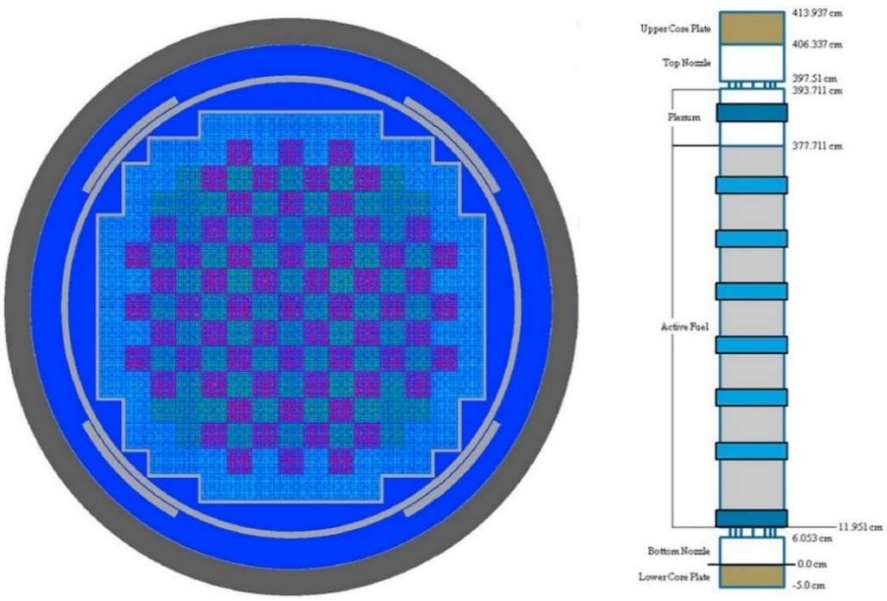

Figure A-1. WBN1 core diagram [A-12].

The WBN1 reactor core encompasses 193 fuel assemblies containing the fissionable material. Each 17 × 17 fuel assembly, which are 12 ft. tall, includes 264 fuel rods, 24 guide tubes, and one central instrumentation tube. The reactor core is loaded with three regions of fuel assemblies with specific enrichments of 2.11%, 2.619%, and 3.10%, as shown in Figure A-1. The design and operational parameters of the WBN1 Cycle 1 are given in Table A-1. The core consists of eight control rod bank clusters (e.g., A, B, C, D, and shutdown banks SA, SB, SC, SD) whose positions are shown in Figure A-2.

The fuel assembly design consists of a 17 × 17 lattice of fuel rods. The fuel assembly is 215 mm wide and is 4063.37 mm in length. It is composed of 264 fuel rods arranged on an orthogonal array with eight spacer grids. The center of the assembly contains a central instrumentation thimble, which provides a channel for the insertion of an in-core neutron detector. In other guide tube positions, there are burnable poison rods consisting of Pyrex and wet annular burnable absorber (WABA) burnable absorbers. Table A-2 summarizes fuel assembly geometry.

Table A-1. Core operating conditions and design parameters.

Description	Value
Rated Core Power (MW)	3411
Reactor System Pressure (MPa)	15.51
Coolant Inlet Temperature (K)	565
Coolant Core Bypass Flow Rate (%)	9
Cycle 1 HZP BOC ARO Critical Soluble Boron Concentration (ppm)	1291
RCCA Control Bank Overlap (Steps)	128
Cycle 1 Uranium Fuel Loading (MT)	88.808
Rated Coolant Total Flow Rate (kg/s)	18231.89
Cycle 1 EOC Exposure (GWd/MT)	16.939

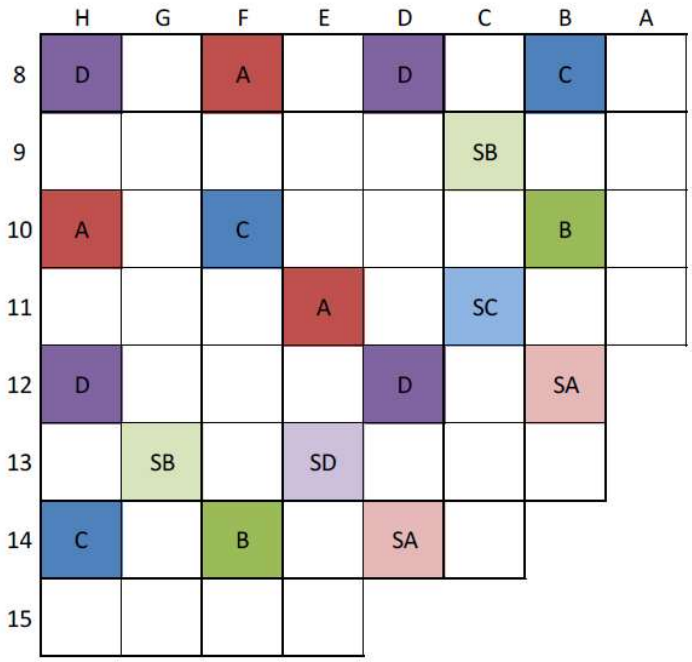

Figure A-2. Core RCCA bank positions (in quarter symmetry) [A-12].

Table A-2. Fuel assembly geometry specifications.

Input	Value
Assembly Pitch (cm)	21.50
Total Assembly Height (cm)	406.337
Fuel Rod Height (cm)	385.10
Rod Pitch (cm)	1.26

A-1.2.2 Benchmark Cases

The cases used in this study are taken from the benchmark exercises detailed in the VERA benchmark specifications [A-13]. However, some modifications have been made to some of the problems for consistency, reproducibility, and simplicity of the study. The cases and their descriptions are outlined in the subsections below.

Case 1: 2D HZP BOC Pin Cell

This case is derived from Problem #1 in [A-13] and demonstrates the code's capability to solve a simple 2D pin cell eigenvalue problem. The boundary conditions for the neutronics calculations are radially reflective. A visual representation of the geometry is shown in Figure A-3. Full specifications and operating conditions are given in Table A-3 and Table A-4, respectively. The problems present a range of fuel temperatures under full operating and isothermal conditions typical of zero power conditions at an NPP. In addition, these pin cell problems describe a heterogeneity of the fuel, gas gap, cladding, and moderator with the final problem (e.g., 1E), which is indicative of an Integral Fuel Burnable Absorber (IFBA) with a thin zirconium coating.

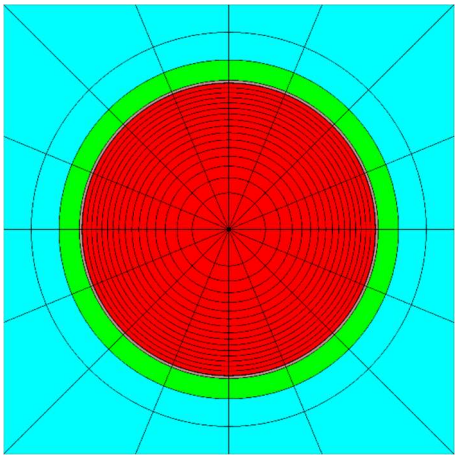

Figure A-3. Radial geometry for Case 1.

Table A-3. Pin cell specifications for Case 1.

Specification	Value
Fuel pin radius	0.4096 cm
Inner clad radius	0.418 cm
Outer clad radius	0.475 cm
Fuel enrichment	3.1%
Fuel density	10.257 g/cm^3

Table A-4. Operating conditions for Case 1.

Problem	Moderator Temperature (K)	Fuel Temperature (K)	Moderator Density (g/cm^3)
1A	565	565	0.743
1B	600	600	0.661
1C	600	900	0.661
1D	600	1200	0.661
1E	600	600	0.743

Case 2: 2D HZP BOC Lattice

Derived from Problem #2 in [A-13], this problem demonstrates the modeling of a simple 2D array of fuel rods typical of central assembly in an NPP reactor core. Boundary conditions are radially reflective; the lattice geometry is described in Figure A-4. The fuel lattices include problems with and without Pyrex (borosilicate glass) poisons. Table A-5 and Table A-6 detail the full specifications and operating conditions with a description of the fuel assemblies, respectively. Additional problems separate from the reference specifications were also introduced in this case. These additional problems include an additional 2.1% and 2.6% enrichment of the fuel, as well as uniform fuel and moderator temperature for the problems involving Pyrex.

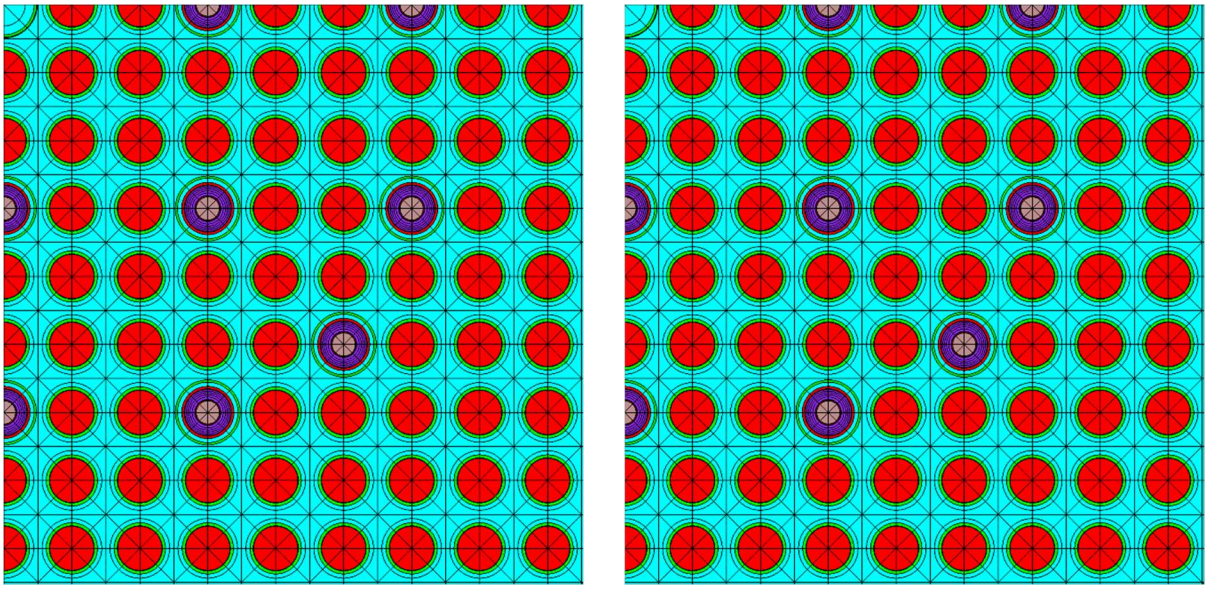

Figure A-4. Radial geometry for Case 2 for problems without Pyrex (left) and with 24 Pyrex (right).

Table A-5. 17 × 17 lattice specifications for Case 2.

Specification	Value
Inner guide tube radius	0.561 cm
Outer guide tube radius	0.602 cm
Inner instrument tube radius	0.559 cm
Outer instrument tube radius	0.605 cm
Inter-assembly half gap	0.04 cm

Table A-6. Operating conditions for Case 2.

Problem	Lattice Configuration and Enrichment (%)	Moderator Temperature (K)	Fuel Temperature (K)	Moderator Density (g/cm^3)
2A – 2.1	2.1	565	565	0.743
2A – 2.6	2.6	565	565	0.743
2A – 3.1	3.1	565	565	0.743
2E – 565	3.1 w/12 Pyrex rods	565	565	0.743
2E – 600	3.1 w/12 Pyrex rods	600	600	0.743
2F – 565	3.1 w/24 Pyrex rods	565	565	0.743
2F – 600	3.1 w/24 Pyrex rods	600	600	0.743

Case 3: 2D HZP BOC Reflector Colorset

Developed as an extension of Problem #2 in [A-13], this case investigates the fuel assembly interfaces and control rod effects in 2D. For the geometry of this calculation, the fuel baffle gap is taken as 0.19 cm, while the baffle thickness is taken as 2.85 cm, and the visual model is shown in Figure A-5. The geometry specification used in this case study is different from the benchmark specification as the there is only a single driver assembly as opposed to the 3 x 3 setup defined in the specification. In addition, the spacer grids are not modeled for this problem either.

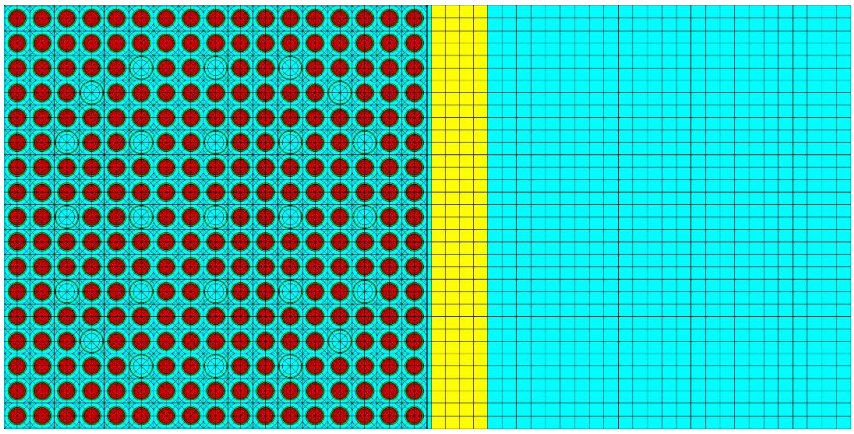

Figure A-5. Radial geometry for Case 3.

Case 4: Physical Reactor Zero Power Physics Tests (ZPPTs)

This problem is based on Problem #5 in [A-13] and it is typical of nuclear core analysis tests. It further demonstrates the prediction of the eigenvalue and core reactivity coefficients without TH feedback or depletion. This problem is associated with the ZPPTs, which are performed at the beginning of fuel cycle startups. The fuel is at HZP isothermal conditions.

Case 5: 3D HFP BOC Physical Reactor

This problem is based on Problem #7 in [A-13] and it is typical of an operating reactor in geometric detail. It further demonstrates equilibrium xenon isotopes and critical soluble boron search with TH feedback to the neutronics in the fuel and the coolant. For this physical reactor, HFP, nominal power, and flow conditions are used and equilibrium concentration of the fission product Xenon calculation and distribution per fuel rod location is used to calculate the power distribution.

A-1.3 Modeling Approach

The modeling of the reactor system and fuel assemblies is similar to the benchmark specifications for both. Despite the benchmark specifications described in the above sections, some approximations and simplifications were made in the final modeling of the pin cell and assemblies for consistency in the comparison calculations. The outlined models are of different fidelities and include the pin cell, assembly, reflector, and full core model. It is noted that the purpose of this benchmark is to identify the most appropriate code for the development of the plant fuel reload optimization framework. More specifications not defined in the above sections can be found in [A-13].

In the pin cell model, no approximations are made to the geometry of this model. The reflector colorset calculation is simplified from the 3 × 3 layout described in the specification to a one 1D driver/reflector configuration. For the full core geometry with the 2.6% and 3.1% enrichment fuel assemblies with burnable poisons, the Pyrex rods modeling for both assemblies are 20 and 16, respectively.

A-1.3.1 VERA-CS

The VERA-CS code sequence used in this work uses MPACT with temperature correction feedback from CTF. VERA's common input is concise and reasonably intuitive and allows for a single reactor core definition to be used for both codes with an elegant transference of variables between codes. MPACT was run with eight radial planes and a ray spacing of 0.05 cm for the MOC solver. The 3D core problems were run with 58 axial planes for a total of 464 cores. Quarter-core symmetry was applied in all instances. While TH coupling with CTF was active for each problem, only Problem #7 returned non-trivial temperature corrections, due to the HFP reactor condition. The same axial plane definitions and input were used in CTF. Fuel temperature corrections to the CTF conductance model were applied from BISON fuel performance simulations done by CASL.

A-1.3.2 SIMULATE-3

The SIMULATE-3 code uses the two-step approach to core analysis. The CASMO-4 2D transport code was used to generate few-group homogenized cross-sections and heterogeneous pin-by-pin form functions, which was used by the CMS-LINK auxiliary code to generate a binary macroscopic cross-section library accessed by SIMULATE-3 for the whole core coupled neutronics TH analysis. The lattice physics calculations at the pin cell and assembly level were performed with CASMO-4 only and used for Cases 1 and 2. CASMO-4 uses a MOC solver carried out in 70 energy groups with effective resonance cross-sections calculated individually for each fuel pin via an equivalence theorem (e.g., rational approximations of the fuel self-collision probability). The 'S3C' card was used in the CASMO-4 input deck to generate a case matrix of calculations (e.g., cross-sections and discontinuity factors) as a functions of fuel temperature, moderator temperature, boron concentration, control rod insertions, and exposure.

The core simulation cases (e.g., Cases 4 and 5) are performed for the SIMULATE-3 code by the modeling of 17 × 17 radial mesh with two radial nodes per assembly and one outer ring of reflector assemblies. Axially, 26 equal nodes were used for the fuel active length and one node for the top and bottom reflectors. Quarter-core symmetry is also applied for all simulations. The two-group QPANDA solution with a conventional cross-section computation was used as the neutronics model for the simulation with the flux and eigenvalue convergence criteria set as 5.0E – 04.100 coupling coefficient iterations per state point were used to solution convergence.

A-1.3.3 PARCS

The PARCS calculation chain involves the cross-section generation with POLARIS in the first step before performing the core calculations in the second step. For Cases 1 and 2, only POLARIS was used, since the calculations involved only 2D lattice calculations at the pin cell and assembly level. The POLARIS MOC solver was used to condense, self-shield, and homogenize the SCALE 56 group ENDF/B-VII.1 cross-section library to the conventional two-group structure. The ESSM is used for the cross-section self-shielding, while for the transport calculation, the MOC BICGSTAB solver is used with 16 azimuthal angles per octant and 0.08 cm spacing between the rays. The scalar flux and k_{eff} tolerance were set to 1E-5. The P1 critical spectrum calculation is performed for only Cases 4 and 5 that require core calculations. The radial mesh discretization used for the fuel pin was one node for the whole fuel rod with eight angular sectors. This POLARIS modeling is considered the low fidelity (LoFi) model that is also used for the cross-section generation for Cases 4 and 5. In Problems #1 and #2, the lattice calculations were performed only for the specific conditions of each exercise, but for the core Cases 4 and 5, the cross-sections were parameterized as a function of the fuel temperature, coolant temperature, boron concentration, and control rod presence. A total of 48 parametric points for all the possible combinations of the following parameters were calculated:

- Fuel temperature: [550K, 900K, 1500K, 2200K]
- Coolant temperature: [550K, 575K, 600K]

- Boron concentration: [0 ppm, 2000 ppm]
- Control rod: [in, out].

These parametric points were computed for each assembly type in the core calculations. For Cases 3, 4, and 5, the reflector calculations were performed additionally by using the same reflector for the radial, top, and bottom locations in the core. Finally, for Cases 1 and 2 that are computationally cheap, a higher fidelity (HiFi) POLARIS model was investigated as well. The HiFi model used the 252g ENDF/B-VII.1 SCALE cross-section library, which is a radial mesh discretization of 16 nodes and 16 angular sectors.

The PARCS modeling of Cases 4 and 5 consist of 17 x 17 radial mesh with one node per assembly and one outer ring of reflector assemblies. Axially, 26 equal nodes were used for the fuel active length and one node for the top and bottom reflectors. The PARCS diffusion multi-group NEM solver was used with convergence tolerances of 1.0E – 06 for the eigenvalue, 5.0E – 05/1.0E – 03 for the global/local fission source, and 1.0E – 03 for the fuel temperature.

A-1.3.4 Results and Analysis

A-1.3.4.1 Lattice Physics Calculations

Lattice physics calculations were performed for the different codes under consideration to generate parameterized cross-section libraries. Stand-alone neutronics core calculations were also performed to further illustrate the code capabilities.

Case 1: 2D HZP BOC Pin Cell

For Case 1, which is a pin cell problem, the parameter under comparison was the effective multiplication factor (k_{eff}). Furthermore, the results of these stand-alone neutronics calculations for the effective multiplication factor are presented in Table A-7. These results also include the reference results reported in [A-13] using the SCALE 6.2 code KENO-VI, which is a continuous energy (CE) Monte Carlo-based transport tool.

The pin cell problems were calculated using VERA-CS, POLARIS, and CASMO. The effective multiplication factor is compared with the reference results calculated by the KENO-VI code from the CASL VERA benchmark. The results of the calculation for the different codes and reference values are listed in Table A-7, with the comparison results presented in Table A-8. Because CASMO-4 uses the ENDF/B-VI.8 library, the results of the reference calculation with both the ENDF/B-VII.0 and ENDF/B-VI.8 libraries are presented here. It can be seen that there is a significant difference between the POLARIS HiFi and LoFi results. With this observation, it can be seen that the code results agree well with the reference results and the errors of the calculation problems are within 205 pcm. The increased difference observed for the 1E problem indicates that there is an issue with the modeling of the IFBA fuel pin with VERA. This significant difference might have dominant contributions from modeling the heterogeneity of the fuel pin rather than the cross-sections calculated for this fuel pin although both are factors for this.

Table A-7. Effective multiplication factor for the 2D HZP BOC pin cell problems.

Codes	CASL-Ref (ENDF/B-VII.0)	CASL-Ref (ENDF/B-VII.0)	VERA	POLARIS-LoFi	POLARIS-HiFi	CASMO
1A	1.18704	1.18336	1.18704	1.18533	1.18643	1.18428
1B	1.18215	1.17855	1.18221	1.18034	1.18194	1.17952
1C	1.17172	1.16811	1.17165	1.16989	1.17166	1.16927
1D	1.16260	1.15922	1.16285	1.16091	1.16283	1.16015
1E	0.77169	0.77033	0.76966	0.76585	0.77144	0.77159

Table A-8. Comparison of effective multiplication factor for 2D HZP BOC pin cell problems.

Codes	VERA	POLARIS-LoFi	POLARIS-HiFi	CASMO
1A	0.14	-170.8	-60.8	91.6
1B	6.12	-180.9	-20.9	96.8
1C	-7.55	-183.2	-6.2	115.6
1D	24.33	-169.3	22.7	92.7
1E	-202.74	-584.1	-25.1	126.1

Case 2: 2D HZP BOC Lattice

Case 2, which is a lattice problem, has the effective multiplication factor (k_{eff}) and the radial pin power distribution as its comparative metrics. The results of the lattice calculations for the k_{eff} parameter are presented in Table A-9. Comparisons for both parameters are made to the results presented in Table A-10. Figure A-6, Figure A-7, and Figure A-8, respectively, provide the results for the problems specific to [A-13].

The fuel lattice problems are calculated using VERA-CS, POLARIS, and CASMO. The effective multiplication factor is compared with the reference results calculated by the KENO-VI code from the CASL VERA benchmark. The results of the calculation for the different codes and the reference values are listed in Table A-9 with the comparison results presented in Table A-10. The comparison is made with the corresponding libraries for the different codes. The results show excellent value agreement for the k_{eff} with the maximum difference of 150 pcm. In addition, a comparison of the pin power distribution with a maximum difference of 2.60%. The CASMO results are consistently higher than the results of the other two codes as well.

Table A-9. Effective multiplication factor for the 2D HZP BOC lattice problems.

Codes	CASL-Ref (ENDF/B-VII.0)	CASL-Ref (ENDF/B-VI.8)	VERA	POLARIS-LoFi	POLARIS-HiFi	CASMO
2A – 2.1	-	-	1.0572489	1.05650	1.05616	1.05323
2A – 2.6	-	-	1.1296893	1.12853	1.12790	1.12566
2A – 3.1	1.182175	1.17852	1.1822784	1.18085	1.18112	1.17824
2E – 565	-	-	1.0272699	1.07078	1.07051	1.06922
2E – 600	1.069627	1.066596	1.0706106	1.06864	1.06815	1.06718
2F – 565	-	-	0.9799487	0.97787	0.97719	0.97645
2F – 600	0.976018	0.973376	0.9775254	0.97471	0.97471	0.97416

Table A-10. Comparison of effective multiplication factor for 2D HZP BOC lattice problems.

Codes	VERA	POLARIS-LoFi	POLARIS-HiFi	CASMO
2A – 3.1	10.34	-132.5	-105.5	-28.0
2E – 600	98.36	-98.7	-147.0	58.4
2F – 600	150.74	-61.8	-130.8	78.4

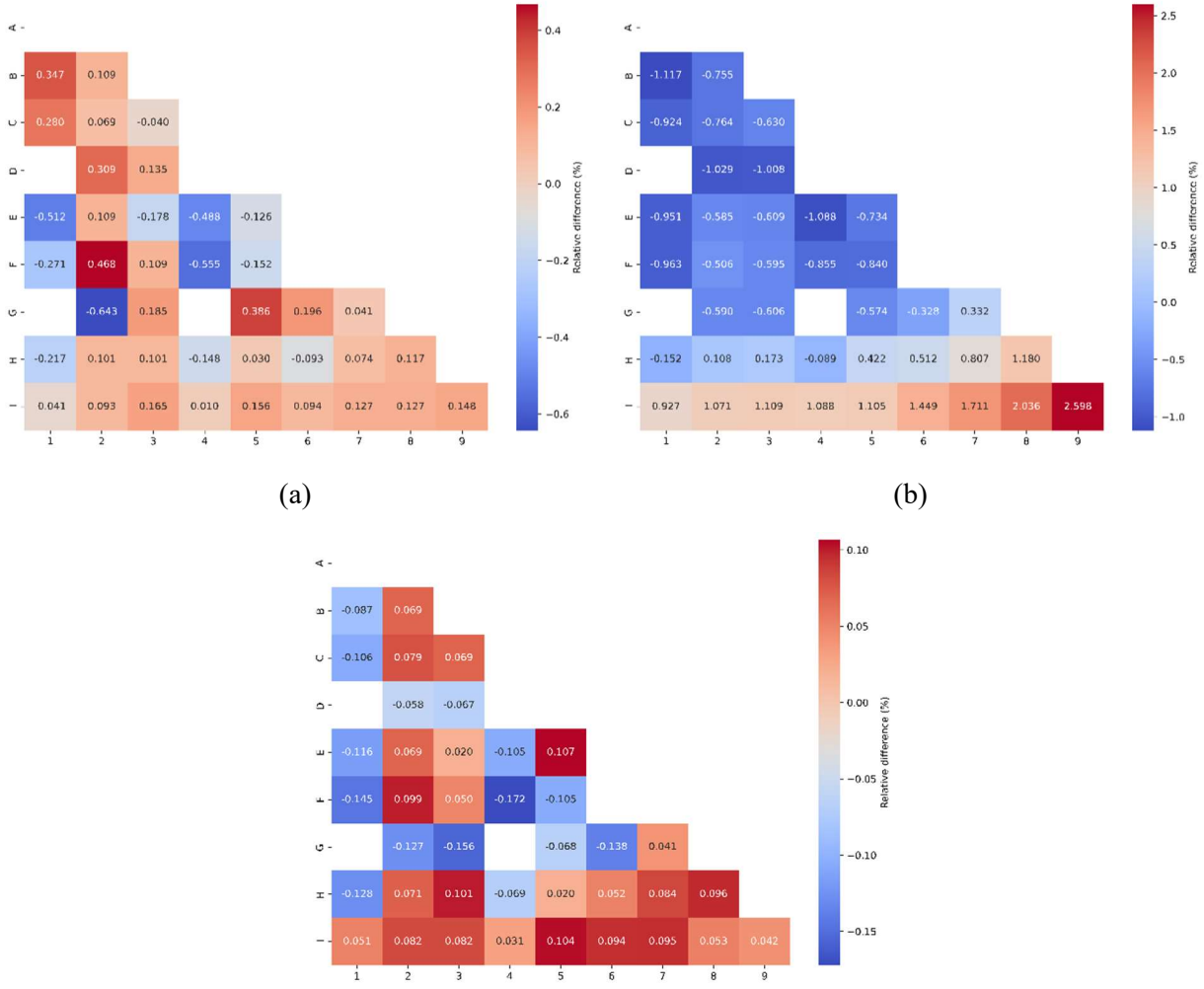

Figure A-6. Comparison of pin power distribution for problem 2A – 3.1 for (a) VERA-CS; (b) CASMO; and (c) POLARIS with CASL reference results.

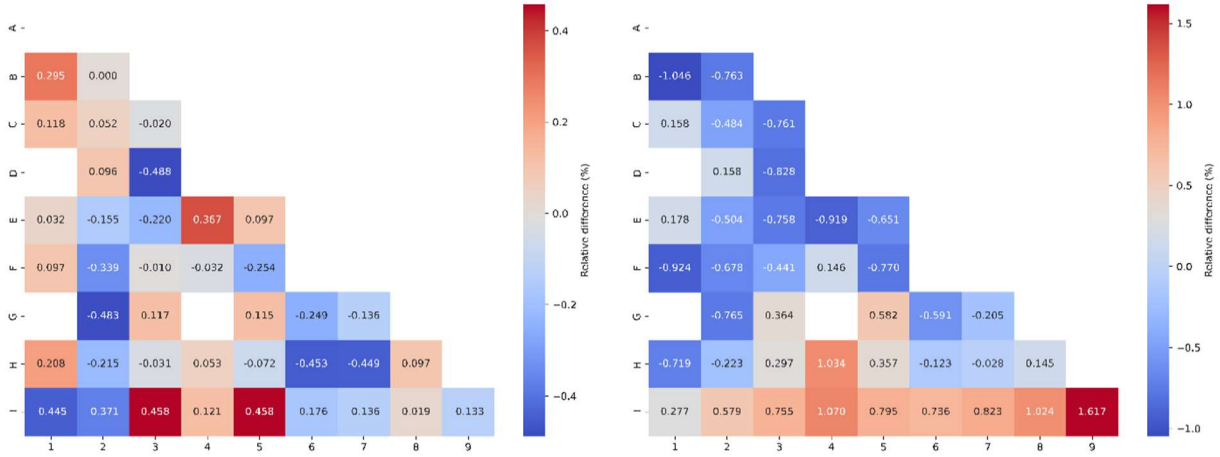

(a)

(b)

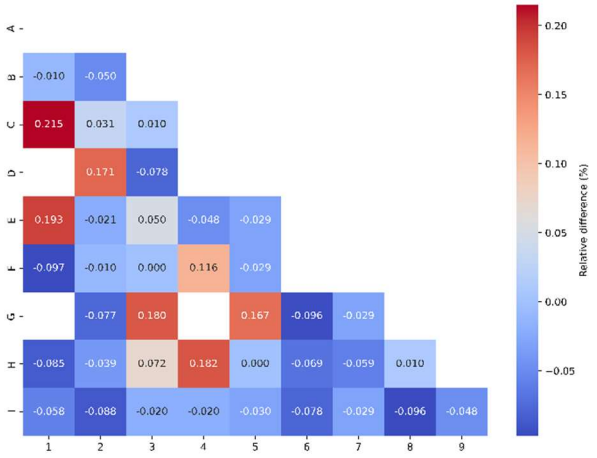

(c)

Figure A-7. Comparison of pin power distribution for problem 2E – 600 for (a) VERA-CS; (b) CASMO; and (c) POLARIS with CASL reference results.

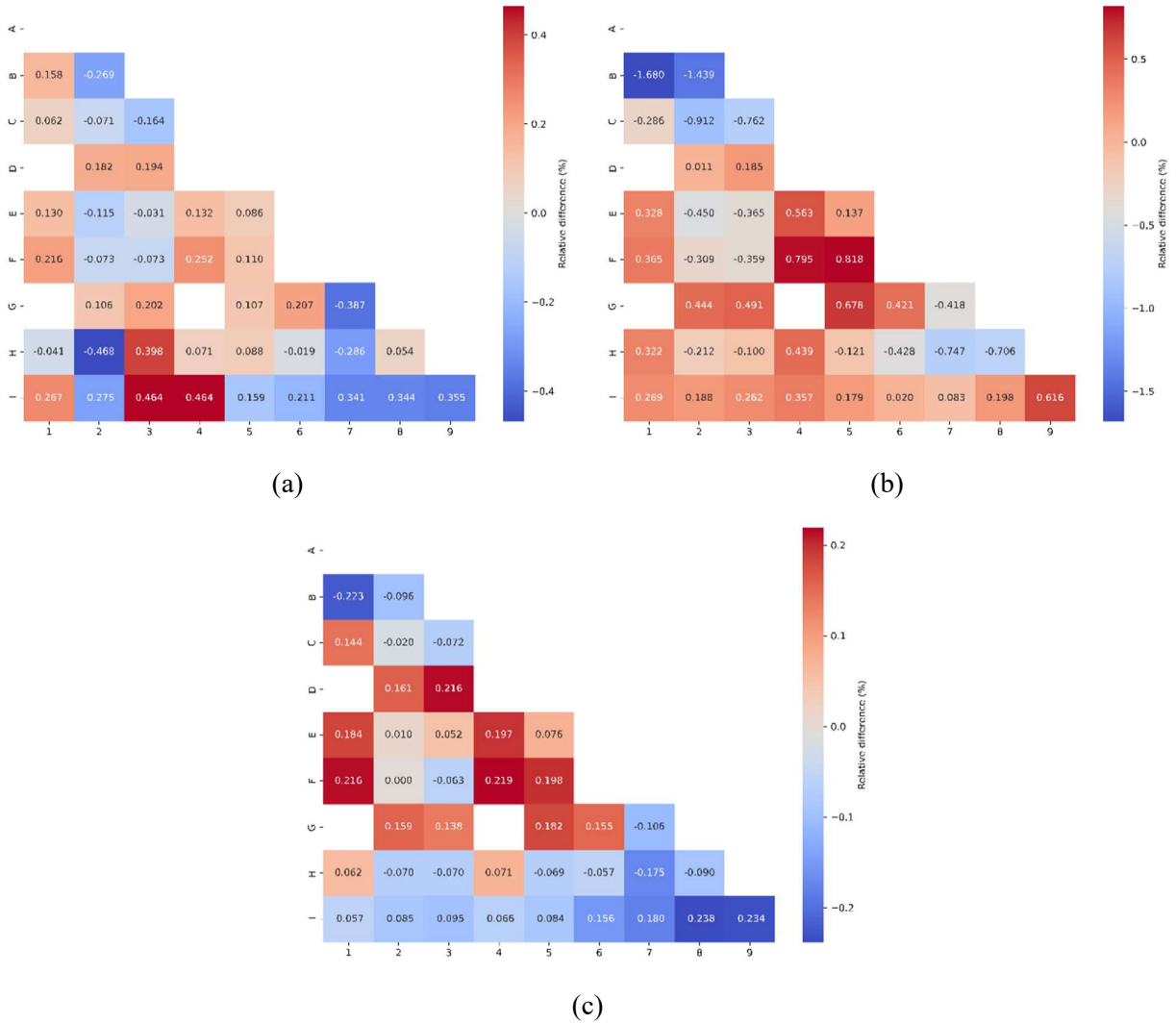

Figure A-8. Comparison of pin power distribution for problem 2F – 600 for (a) VERA-CS; (b) CASMO; and (c) POLARIS with CASL reference results.

Case 3: 2D HZP BOC Reflector Colorset

For this calculation, the parameters in consideration are the two-group cross-sections. The results are presented in Table A-11.

The reflector cross-sections for both the POLARIS and CASMO codes are presented in Table A-11 with no information presented for the VERA code. This is because VERA does not apply the conventional two-step approach to core analysis; rather, the neutronics calculation is performed using a multi-group-based library. From the results, it is observed that the cross-section results for CASMO are consistently higher the POLARIS results. However, the differences are all within reasonable ranges and these discrepancies will be observed in the core calculations.

Table A-11. Reflector two-group cross-sections for the 2D HZP BOC reflector colorset.

	POLARIS		CASMO	
	G1	G2	G1	G2
Total	6.47E – 01	1.87E + 00	6.70E – 01	1.90E + 00
Absorption	2.06E – 03	4.13E – 02	2.70E – 03	4.27E – 02
NuFission	0.00E + 00	0.00E + 00	0.00E + 00	0.00E + 00
Diff. Coefficient	1.32E + 00	2.78E – 01	1.19E + 00	2.70E – 01
In Scattering	6.14E – 01	1.83E + 00	6.42E – 01	1.85E + 00
Out Scattering	3.16E – 02	7.04E – 04	2.58E – 02	1.01E – 03

A-1.3.4.2 Multi-Physics Steady-State Core Simulations

Using the several sets of few-group homogenized cross-sections for each fuel assembly generated from the lattice calculations in the above section, multi-physics steady-state core calculations were performed.

Case 4: Physical Reactor Zero Power Physics Tests (ZPPTs)

Case 4 is a core simulation with the core under HZP conditions. For this problem, the parameters under comparison are the axial and radial power profile distributions. Code-to-code comparison is performed here with the results of the VERA-CS code as a reference to illustrate the relative difference (%) between the codes under consideration. The results for the axial and radial power distribution is shown in Figure A-9, Figure A-10, and Figure A-11, respectively.

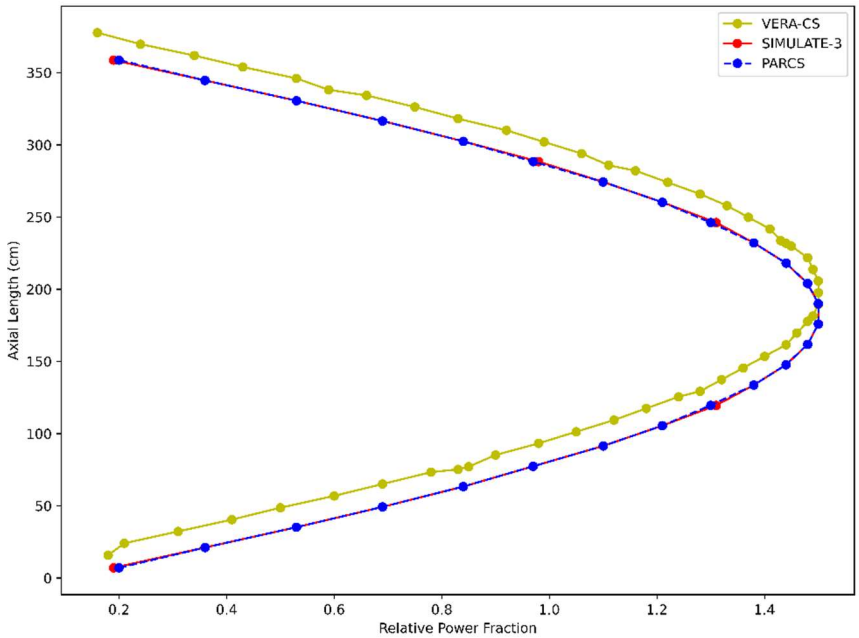

Figure A-9. Axial power profile for Case 4.

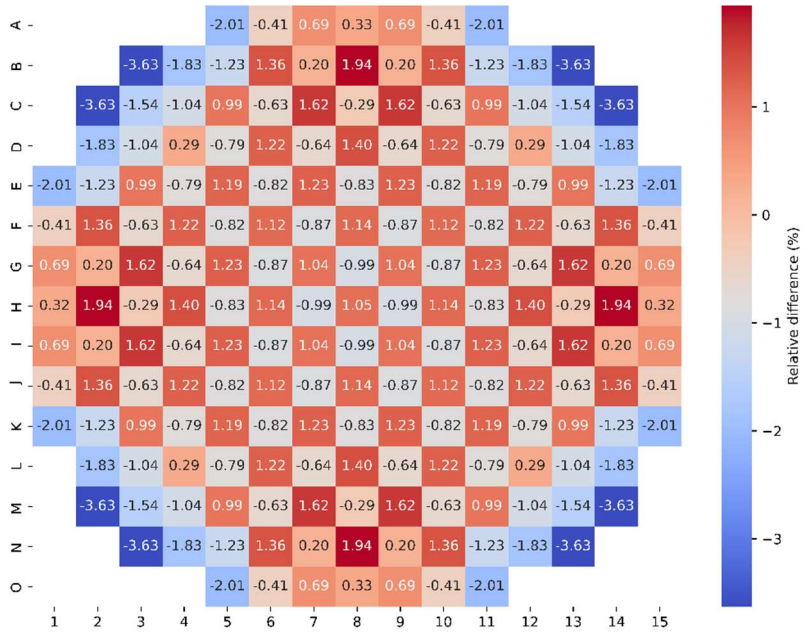

Figure A-10. Case 4 radial power profile comparison of SIMULATE-3 with VERA results.

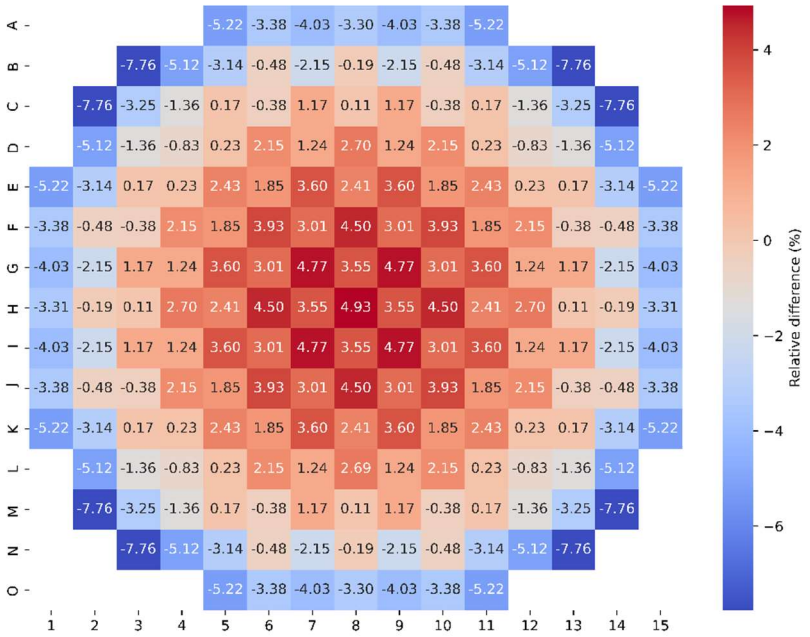

Figure A-11. Case 4 radial power profile comparison of PARCS with VERA results.

An initial comparison of the axial power profile indicates an agreeable response between all three results with SIMULATE-3 and PARCS overlapping each other. Radial comparison of the assembly power indicates that the highest absolute relative difference for both PARCS and SIMULATE-3 are 7.8% and 3.6%, respectively. These maxima are found in the reflector region, which is indicative of the cross-section results obtained in Section A-1.3.4.1. It is important to note that the results obtained here for this simulation has a bias in the nuclear data library. The SIMULATE-3 code uses the ENDF/B-VI.8 nuclear data library, whereas the VERA-CS and PARCS codes use the ENDF/B-VII.0 library.

Case 5: 3D HFP BOC Physical Reactor

For this physical reactor, HFP, nominal power, and flow conditions are used and equilibrium concentration of the fission product Xenon calculation and distribution per fuel rod location is used to calculate the power distribution. The results for the axial and radial power distribution is shown in Figure A-12, Figure A-13, and Figure A-14, respectively. For the HFP simulation, similar trends in the comparison observed in the HZP simulation are also observed here for the axial power profile. However, differences between all three codes are noted here. This is because of the TH model employed in the different codes and their different assumptions and simplifications.

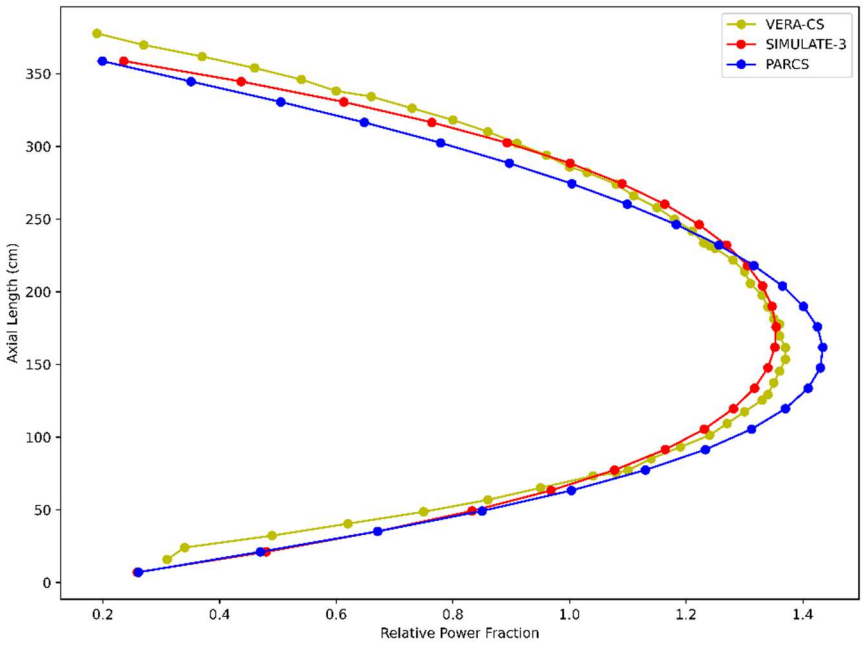

Figure A-12. Axial power profile for Case 5.

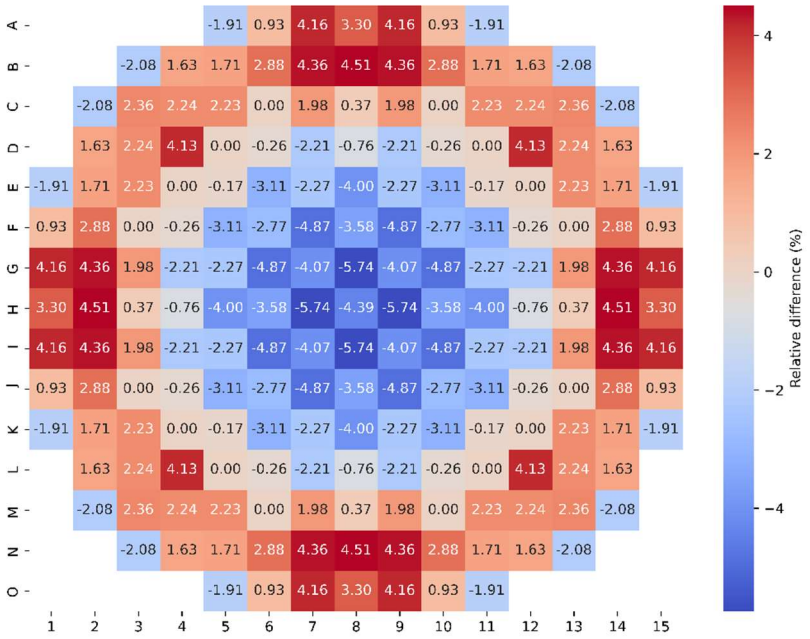

Figure A-13. Case 5 radial power profile comparison of SIMULATE-3 with VERA results.

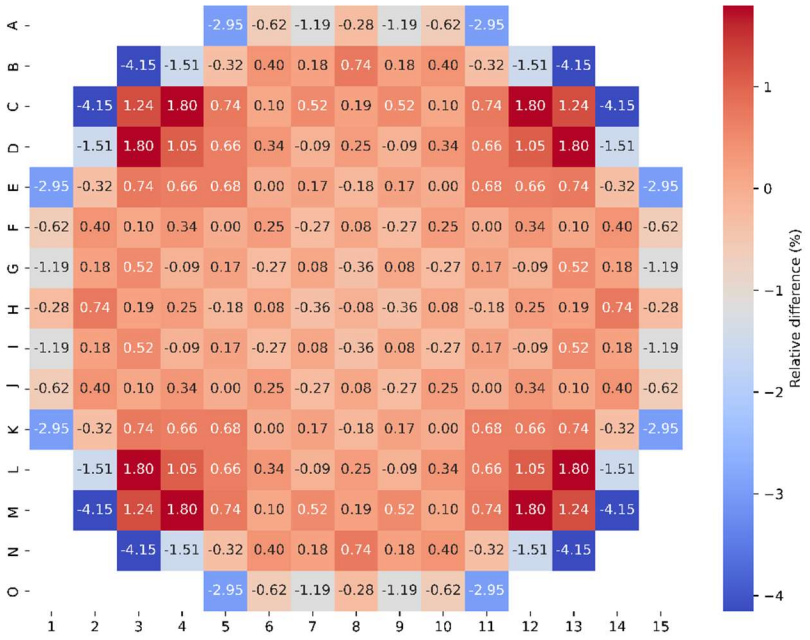

Figure A-14. Case 5 radial power profile comparison of PARCS with VERA results.

To understand the impact of the assumptions and approximations made in the lower-order solver PARCS and SIMULATE-3 on the TH parameters, the axial profile of the fuel temperature and moderator density are plotted, as shown in Figure A-15 and Figure A-16, respectively. Large differences can be seen in the comparison in both cases. For the fuel temperature distribution, although the SIMULATE-3 results agree well with VERA, it is obvious that it fails to capture the space grid effects (e.g., a series of dips on the curve). In the comparison of the moderator density, the VERA results present a relatively large value in the hot channel, indicating that the cross flow modeled by the subchannel code leads to lower coolant temperature, and thus, higher density.

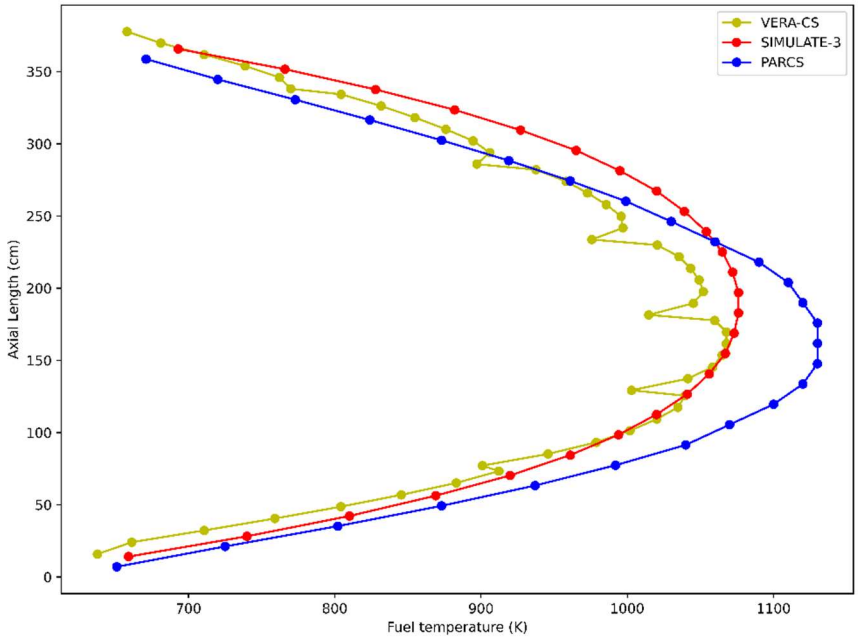

Figure A-15. Axial fuel temperature profile for hot assembly/channel.

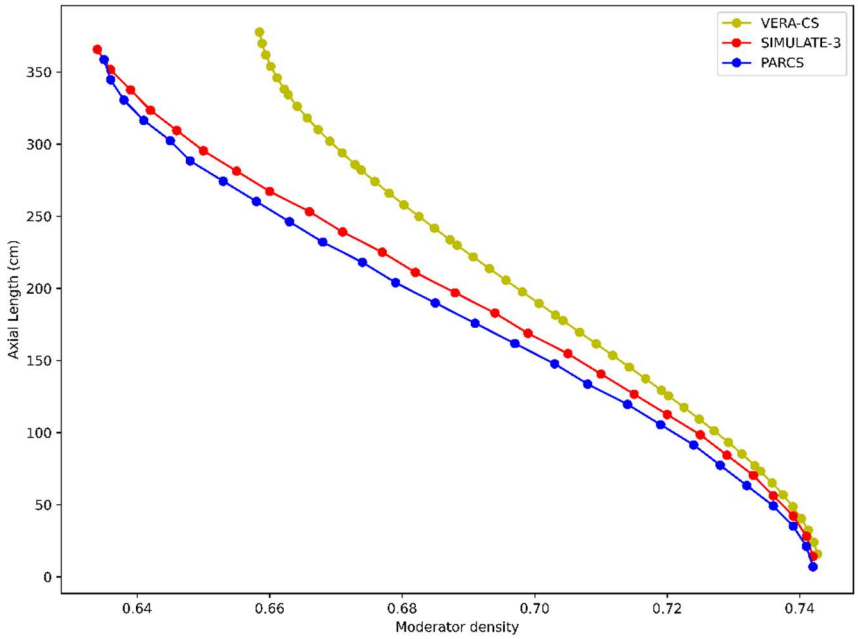

Figure A-16. Axial moderator density profile for hot assembly/channel.

A-1.3.4.3 Physics and Performance Comparison

Although the accuracy of the simulations is an important metric by which the efficiency of the different codes is compared, it is not the only important metric for choosing the optimal code for the optimization problem. Some other metrics that were considered include qualitative metrics like modeling effort, code capability, and license, as well as another quantitative metric like the computational cost to the system. Here, the computational cost is formulated as total central processing unit (CPU) runtime so that the impact of parallel computing is mitigated.

In terms of the modeling effort required, all three codes showed an ease of input definitions with predefined variables making for a concise input of parameters. However, as noted in previous sections, the nuclear data libraries used in the different code versions here are different. The SIMULATE-3 code uses data from an older nuclear data library known as the ENDF/B-VI.8 library, while the VERA-CS and PARCS codes used the relatively newer nuclear data library, ENDF/B-VII.0. Although the information contained in both libraries are different, it is observed from the differences in the axial and radial power profiles are within an acceptable range. The three codes also model the entirety of the reactor system including, but not limited to, spacer grids. Also, the different codes can be employed for fuel management, core follow, and reload analysis of the reactor system. Finally, all three codes are held under license agreement, but are available on the North Carolina State University RDFMG cluster.

The CPU runtime for the different cases is reported in Table A-12. Here, since the VERA-CS code does not have the lattice physics option, there is no value reported for these cases. Rather, a single value is reported for the HZP and HFP core simulations.

In the comparison of the CPU runtime, it is clear at a glance that the simulation results obtained with VERA-CS have the longest runtime. However, it should be noted that for the two-step approach codes, Cases 1, 2, and 3 have to be run multiple times for a range of reactor conditions to fully characterize the reactor core simulation. This does increase the computational time for the lattice physics calculations; however, for fuel reload optimization purposes, only the core simulation has to be run repeatedly. The increased runtime observed for Case 3 is a result of the increased discretization of the reflection region required by the POLARIS code for accurate representation of the assembly discontinuity factors (ADFs).

Table A-12. CPU runtime comparison for the different codes.

Cases	VERA-CS runtime (hh:mm:ss)	POLARIS/PARCS runtime (hh:mm:ss)	CASMO-4/SIMULATE-3 runtime (hh:mm:ss)
1	00:00:02	00:00:11/--	00:00:01/--
2	--	00:01:00/--	00:00:05/--
3	--	00:55:00/--	00:00:35/--
4	20:44:15	01:30:00/00:00:02	--/00:00:14
5	45:01:14	01:30:00/00:00:02	--/00:00:07

A-2. Fuel Performance Codes: TRANSURANUS and BISON

Two fuel performance tools—TRANSURANUS and BISON—were used for the benchmark. Similar to core design tool benchmark, the main parameter of interest is simulation time capability, computational efficiency, integration with plant reload optimization framework including RAVEN and RELAP5-3D, and user-friendliness, as well as ATF applicability.

Two well-controlled benchmark cases are used—IFA-432 Rod 3 and IFA-650.2 Rod 2 of OECD/NEA's IFPE program—which is a public domain database on nuclear fuel performance experiments for the purpose of code development and validation [A-14]. These test sets were used for BISON code validation. The IFPE program aims to provide a comprehensive and well-qualified database on Zr-clad UO_2 fuel for model development and code validation in the public domain. The data encompasses both normal and off-normal operation and include prototypic commercial irradiations, as well as experiments performed in Material Testing Reactors. This work is carried out in close cooperation and coordination between the OECD/NEA, International Atomic Energy Agency (IAEA), and Halden Reactor Project.

A-2.1 Description of Fuel Performance Codes

A-2.1.1 TRANSURANUS

TRANSURANUS is a fuel performance code developed at the Joint Research Centre's (JRC's) Institute for Transuranium Elements (ITU) in Karlsruhe, Germany [A-15]. The code approximates the fuel rod behavior with an axisymmetric, axially stacked, one-dimensional radial representation, often referred to as 1.5-D. The code can be employed for both steady-state and transient analyses and incorporates models accounting for the different and interrelated phenomena occurring in the fuel rod. The modeling of fission gas behavior is a crucial aspect of nuclear fuel analysis in view of the related effects on the thermo-mechanical performance of the fuel rod, which can be particularly significant during transients. The TRANSURANUS code can deal with a wide range of different situations, as given in experiments, under normal, off-normal, and accident conditions. The time-scale of the problems to be treated may range from milliseconds to years. The code has a comprehensive material data bank for oxide, mixed oxide, carbide, and nitride fuels, Zircaloy and steel claddings, and several different coolants. It can be employed in two different versions—as deterministic and as a statistical code.

A-2.1.2 BISON

BISON is a finite element-based nuclear fuel performance analysis code applicable to a variety of fuel forms including LWR fuel rods, tri-structural isotropic (TRISO) particle fuel, and metallic rod and plate fuel [A-16]. It solves the fully-coupled equations of thermo-mechanics and species diffusion for either 1D spherical, 1D axisymmetric, 2D axisymmetric, 2D Cartesian, or 3D geometries. Fuel models are included to describe temperature and burnup dependent thermal properties, fission product swelling, densification,

thermal and irradiation creep, fracture, and fission gas production and release. Plasticity, irradiation growth, and thermal and irradiation creep models are implemented for clad materials. Models are also available to simulate gap heat transfer, mechanical contact, and the evolution of the gap/plenum pressure with plenum volume, gas temperature, and fission gas addition. BISON is based on the MOOSE framework and can therefore efficiently solve problems using standard workstations or very large high performance computers.

A-2.2 Benchmark Specifications

Two test sets were selected from BISON standard validation suites [A-16]: (1) IFA-432 test for fuel performance at long-term LWR operation; and (2) IFA-650.2 test for fuel failure mechanism during LOCA.

A-2.2.1 IFA-432 Rod 3

The IFA-432 experiment was part of an effort by the NRC to obtain well-characterized experimental data under conditions that simulate long-term steady LWR operation [A-16]. IFA-432 was a heavily instrumented fuel assembly irradiated in the Halden BWR from 1975 to 1976. The main objectives of IFA-432 were measurements of fuel temperature response, fission gas release, and mechanical interaction on BWR-type fuel rods up to high-burnup. The major FOM is the fuel centerline temperature. During the Halden reactor experiment, the fission gas release threshold was not excessed, except at the peak power position near 28MWd/kgUO_2. For Rod 3 test, the total amount of gas release was low and there was no evidence of thermal feedback while other tests, such as the Rod 1, 2, 5, and 6 Cases, showed a large amount of fission gas release and thermal feedback effect. Fuel temperatures at constant power increased steadily throughout the test.

The test rods initially contained fresh fuel and were operated at power levels near the upper bound for full-length commercial fuel rods. The IFA-432 assembly included six instrumented rods, each with centerline temperature instrumentation in both the top and bottom ends of the fuel column. Three of the six rods (Rods 1, 2, 3) are the focus of this assessment. The IFA-432 assembly also contained neutron detectors, coolant thermocouples, a coolant flow meter, and a transducer to measure internal rod pressure. Three test rods considered here were designed to simulate BWR-6 rod cladding material and dimensions and included only differences in fuel-cladding gap width. Table A-13 shows test rod specifications of IFA-432 test. During the test, the measured maximum temperature was 1800C°. The measured lower-level thermocouple temperatures remained below 1300C°. Rod 3 achieved burnup of approximately 45MWd/kgU. Rod 3 also experienced power ramps in the range of 30-45kW/m. More detail is available on the BISON webpage [A-17].

Table A-13. IFA-431 test rod specifications.

Fuel Rod	Measurement	Unit
Overall length	0.635	m
Fuel stack height	0.5791	m
Nominal plenum height	25.4	mm
Number of Pellets per Rod		
Rod 1	45	mm
Rod 2	44	mm
Rod 3	44	mm
Fill gas composition	He	
Fill gas pressure	0.1	MPa
Fuel	Measurement	Unit
Material	UO_2	
Enrichment	10	%
Density	95	%
Inner diameter	1.752	mm
Outer Diameter	Measurement	Unit
Rod 1	10.681	mm
Rod 2	10.528	mm
Rod 3	10.858	mm
Pellet geometry	flat end	
Grain diameter	22 – 77	μm
Cladding	Measurement	Unit
Material	Zr-2	
Outer diameter	12.789	mm
Inner diameter	10.909	mm
Wall thickness	0.94	mm

A-2.2.2 IFA-650.2 Rod 2

Also performed at the Halden reactor, the IFA-650 tests are the series of integral in-pile experiments to investigate fuel behavior under LOCA conditions [A-18]. The IFA-650 tests focused on embrittlement and mechanical properties of high-burnup cladding. The IFA-650 test series is one important experiment to support the high-burnup fuel design and test of new cladding material validation and verification (V&V) during LOCA. The parameters of interest for the related LOCA are:

- Rod internal pressure (RIP) evolution during the LOCA event
- Fuel rod burst phenomena and cladding deformation.

The second trial test run in IFA-650.2 was performed in May 2004. The main purpose of the IFA-650.2 Rod 2 test was to practice the test case with ballooning and fuel failure to find out how to run the later experiments with the pre-irradiated rods. The test was carried out using a fresh, pressurized PWR rod and low fission power to achieve the desired temperature conditions. The rod plenum volume was made relatively large to be able to maintain stable pressure conditions during ballooning. The target PCT of 1050°C was reached and clad ballooning and rupture occurred at ~800°C. The fabrication characteristics of the IFA-650.2 fuel rod are reported in Table A-14. The fuel rod was located in a standard high-pressure flask in the IFA-650 test rig, which was connected to a high-pressure heavy water loop and a blowdown system.

Table A-14. Design data of IFA-650.2 fuel rod.

Fuel Rod	Material	Unit
Fuel material	UO_2	
Fuel density	95.0	%TD
U-235 enrichment	2.0	wt.%
Active stack length	500	mm
Pellet OD	8.29	mm
Pellet ID	0	mm
Cladding material	Zy-4	
Cladding ID	8.36	mm
Cladding OD	9.50	mm
Diametral gap	70	μm
Free volume	17.4	cm^3
Fill gas	He	
Fill gas pressure	4.0	MPa

During normal operation prior to the test, the rig was connected to the loop. Then, the rig was bypassed, and the LOCA was initiated by opening the valves leading to the blowdown tank. The initial pressure in the loop was ~7 MPa and the counterpressure in the blowdown tank was ~0.2 MPa. During the LOCA phase, a low fission power of 2.3 kW/m was used to achieve the desired temperature conditions. A heater surrounding the rod was used to simulate the heat from adjacent rods. Cladding rupture occurred at ~800°C cladding temperature. The Halden IFA-650.2 test was selected for comparative fuel performance modeling in the IAEA FUMEX-III Project and is being considered also within the IAEA FUMAC Project on Fuel Modeling under Accident Conditions [A-19].

A-2.3 Simulation Environment

All benchmark calculations were executed in both Windows and Linux environments.

A-2.3.1 TRANSURANUS

TRANSURANUS Version 1 Mod1 was used for both the Windows and Linux environment with the following computer configurations:

- **Linux**

  Processor: Intel(R) Xeon(R) CPU E5-2697 v4 @ 2.30GHz

  RAM (GB): 32

- **Windows**

  Processor: Intel(R) Core(TM) i7-9750H CPU @ 2.60GHz

  RAM (GB): 32

Due to the irradiation histories of IFA-432 and IFA-650.2 that have very high level of detail, the simulation time was measured longer than general TRANSURANUS simulation. Table A-15 shows TRANSURANUS computational details for both a Windows and Linux environment. It is noted that generic fuel reload licensing analysis has an order of 100 timesteps, which takes a few seconds of run time.

Table A-15. CPU runtime comparison for the different codes.

Test Case	Operating System	Run Time [s]	Time Step
IFA-432 Rod 3	Windows	27.629	14685
	Linux	54.239	
IFA-650.2 Rod 2	Windows	19.483	3001
	Linux	37.998	

A-2.3.2 BISON

BISON version is controlled by GitLab repository. Table A-16 summarizes the BISON and MOOSE version codes and related Linux library used for benchmark.

Table A-16. BISON, MOOSE, and Linux library version.

Software	Version
BISON	Derived from v1.5, git commit d5d2b4e83 on 2020-11-14
MOOSE	Git commit 7dba80f589 on 2020-11-05
LibMesh	4f3fa5a6a2104ab8784a6519677589738b9aef6f
PETSc	3.10.5

BISON was run under the high performance computing (HPC) cluster at INL. Each test used 32 computer processors in HPC with the execution times given in Table A-17. The BISON IFA-432 Rod 3 test case only includes first eight hours of transient while the entire experiment includes data for 70,000 hours. Considering that BISON can simulate one hour in about 50 seconds of running time, 70,000 hours will need more than 30 days of running time. Hence, no additional BISON simulation was conducted for the IFA-432 Rod 3 test.

Table A-17. BISON simulation execution time.

Test	Operating System	Run Time [s]
IFA-432 Rod 3	Linux	6030
IFA-650.2 Rod 2	Linux	409.8

A-2.4 Result and Analysis

A-2.4.1 IFA-432 Rod 3 Test

The benchmark mainly focused on code capability for predicting the fuel centerline temperature. Only TRANSURANUS was used, and the results were compared with the experimental data. The BISON simulation was not available due to the expected simulation running time needing more than 30 days.

The TRANSURANUS simulation generally agrees with the experimental data. Figure A-17 is the centerline temperature during the entire lifetime. Both the experiment and TRANSURANUS simulation results are very much overlapped and it is not easy to understand the difference. Hence, the ratio between the TRANSURANUS simulation and the experimental data is shown in Figure A-18. It was found that the TRANSURANUS simulation slightly overestimates the centerline temperature mostly at higher temperature range. Figure A-19 shows evolution of gap width evaluation capability of the TRANSURANUS simulation.

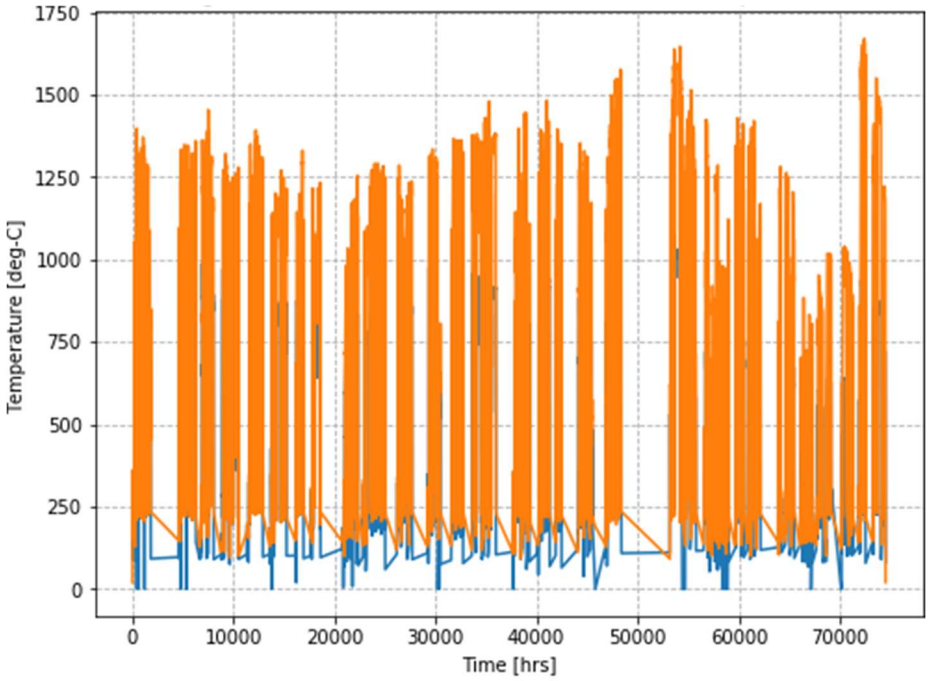

Figure A-17. Centerline temperature of experiment (orange line) and TRANSURANUS (blue line).

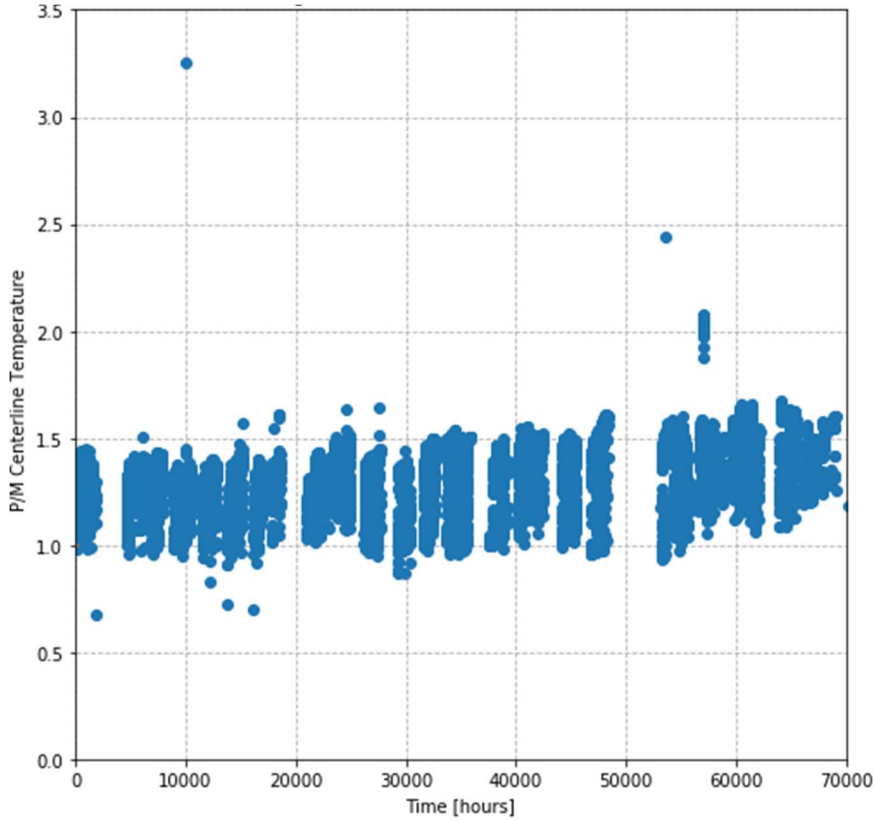

Figure A-18. Ratio of centerline temperature between TRANSURANUS and experiment (P/M = TRANSURANUS results / Experiment data).

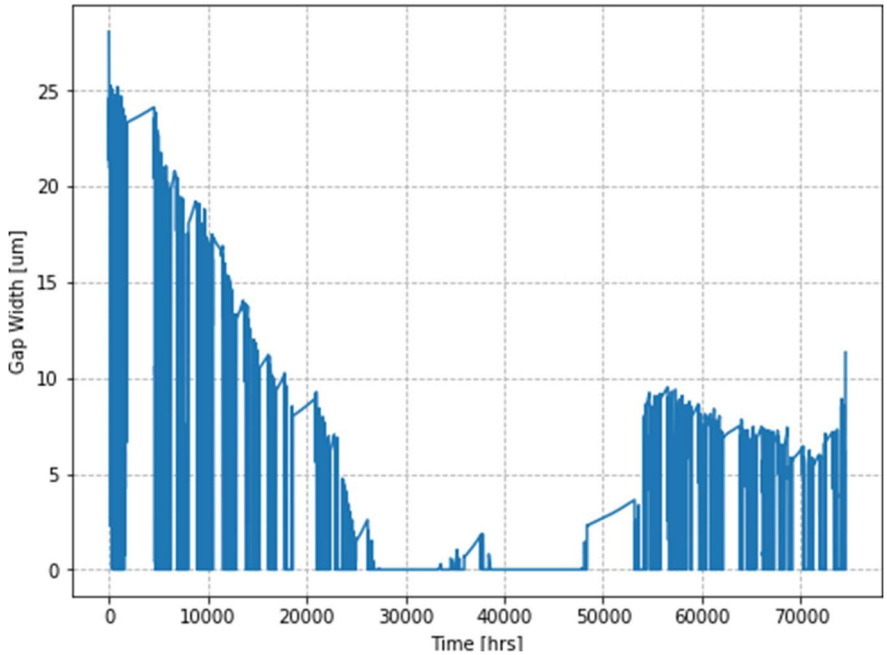

Figure A-19. Gap width inside of the Rod 3 results from TRANSURANUS.

A-2.4.2 IFA-650.2 Rod 2 Test

Both TRANURANUS and BISON were used for the IFA-650.2 Rod 2 test to evaluate rod burst (e.g., ballooning and failure) during the LOCA scenario. The test was carried out using low fission power to achieve the desired conditions for ballooning. Fuel failure occurs due to fuel rod overheating during LOCA and continuous mechanical loading to fuel rod induces large plastic deformation and burst of the cladding. The main cause of fuel rod burst is RIP, as shown in Figure A-20. The RIP increases as LOCA event starts from time 0second. The RIP increases until 7MPa and blowdown to ambient pressure near 61hours of simulation time, which represent fuel rod burst. These phenomena are clearly observed in both TRANSURANUS and BISON simulation. It is noted that experimental pressure gauge instrument has a lower measuring limit of 5.5MPa, while the experiment data line shown as orange in Figure A-20 does not show a limit any smaller than 5.5MPa. Compared to TRANSURANUS, BISON underpredicts pressure during the simulation. Fuel burst time is within 0.1 sec between the experiment and both simulations.

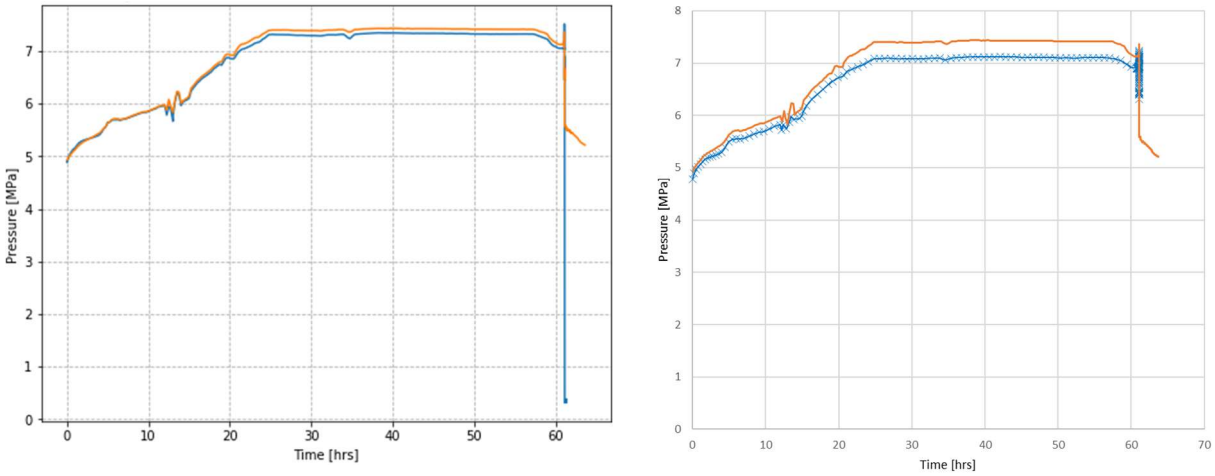

Figure A-20. RIP of TRANSURANUS (left blue), BISON (right blue), and experiment (orange).

A-3. Concluding Remark

The main purpose of this benchmark study was to review available computational tools to be used in plant reload optimization framework development. The selection of the tools is purely based on applicability to the optimization framework. The main criteria of tool selection are as follows.

- Computational speed: Optimization algorithm (e.g., GA) requires a minimum order of hundreds of simulations. Hence, the tools need to be run fast as possible, preferably in order of 10th of seconds.
- Higher technical maturity: Optimization framework aims at immediate industrial deployment. The tools under the framework need to have at least higher than TRL level 7[3].
- Coupling with RAVEN: RAVEN is the main software to control the optimization part of the framework. Though RAVEN has a high degree of freedom, code coupling with RAVEN needs to be verified.
- ATF and/or high burnup: The tools under the optimization framework need to address the capability to apply both ATF and high burnup operation.

[3] TRL is from 1 to 9, Level 7 is minimum requirements for actual demonstration, https://www.nasa.gov/directorates/heo/scan/engineering/technology/technology_readiness_level

- PWR and BWR: The tools under the optimization framework need to be applicable for both PWR and BWR.

For the core design tool, the result of this study shows that the two-step approach code with the core simulation and the reactor analysis is more favorable to optimization studies than one-step approach code. The main benefit of two-step approach code is the ease of repeatability. As a result, CASMO/SIMULATE is the best option for the optimization framework in terms of above criteria.

For the fuel performance analysis tool, TRANSURANUS has a higher advantage or simulation time, which shows more than a hundred times faster than BISON while requiring comparably lighter computational resources. The fast execution time of TRANSURANUS also eliminates the need for simulating with ROM.

A-4. Additional Figures

Although the comparison of the results from the different codes are presented in the previous results section, it is important to report the central values from which those comparative metrics are derived to have a better understanding of the results. The radial power profile plots for Case 4 and Case 5 are presented here.

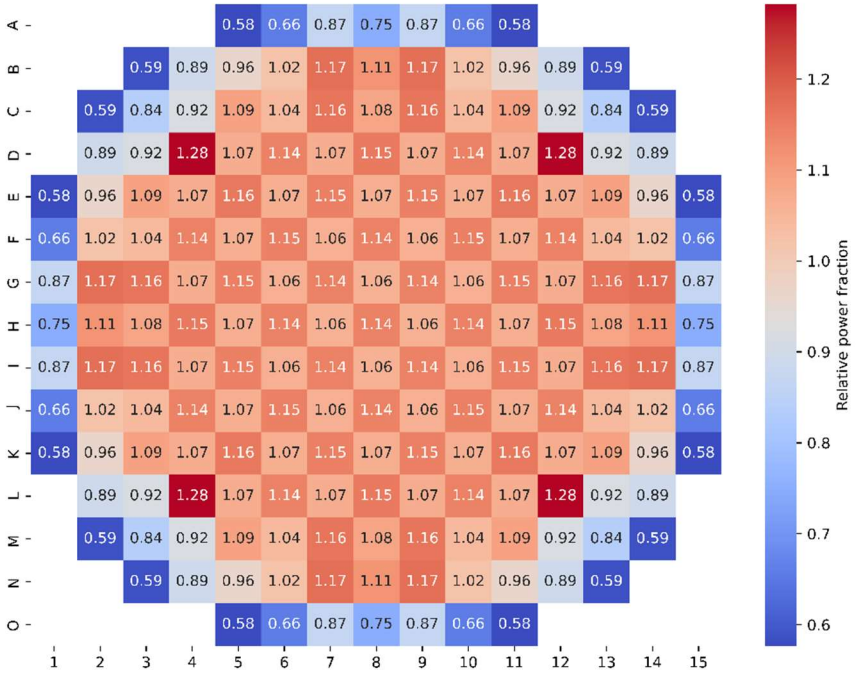

Figure A-21. Radial power profile for Case 4 with VERA-CS.

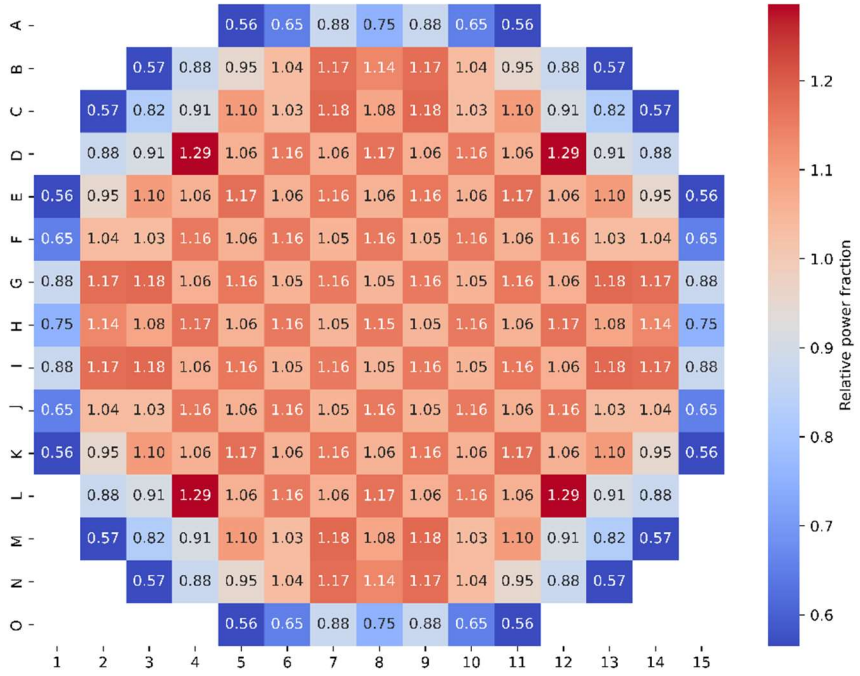

Figure A-22. Radial power profile for Case 4 with SIMULATE-3.

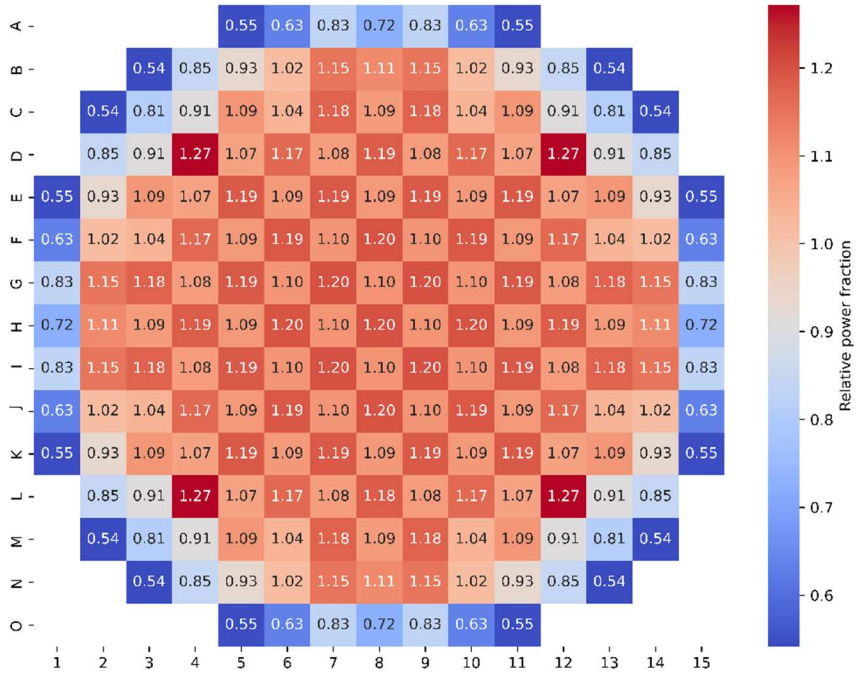

Figure A-23. Radial power profile for Case 4 with PARCS.

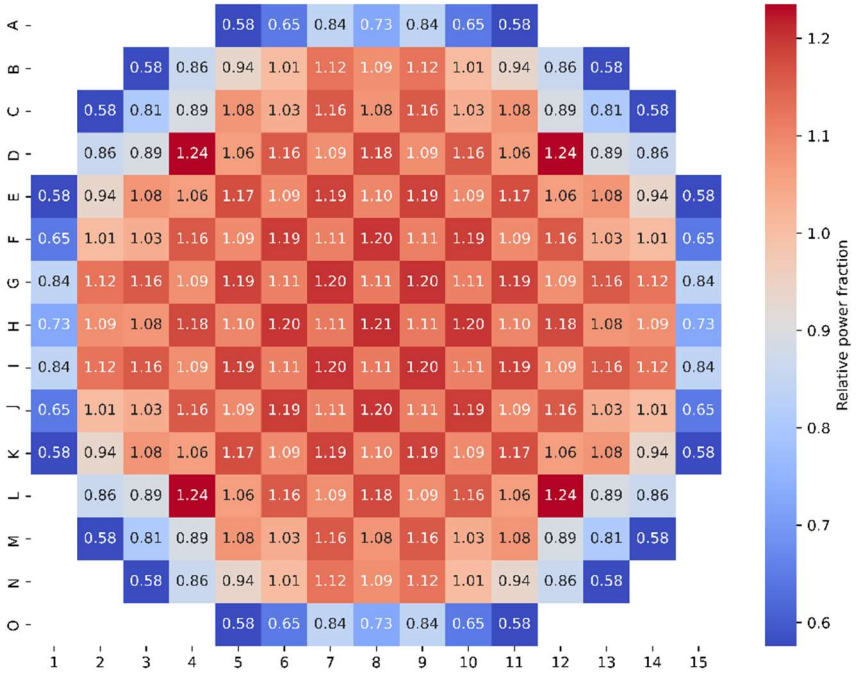

Figure A-24. Radial power profile for Case 5 with VERA-CS.

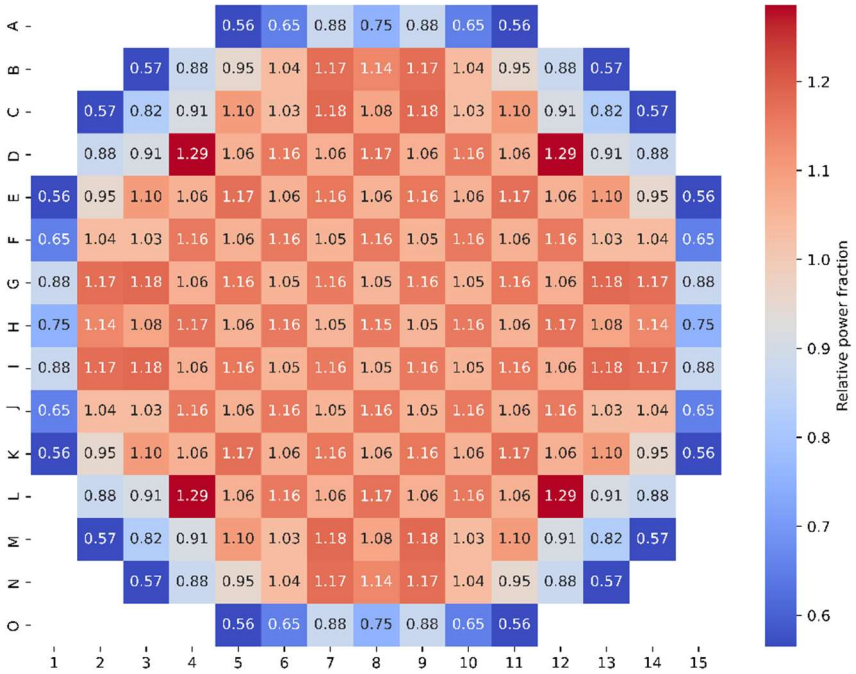

Figure A-25. Radial power profile for Case 5 with SIMULATE-3.

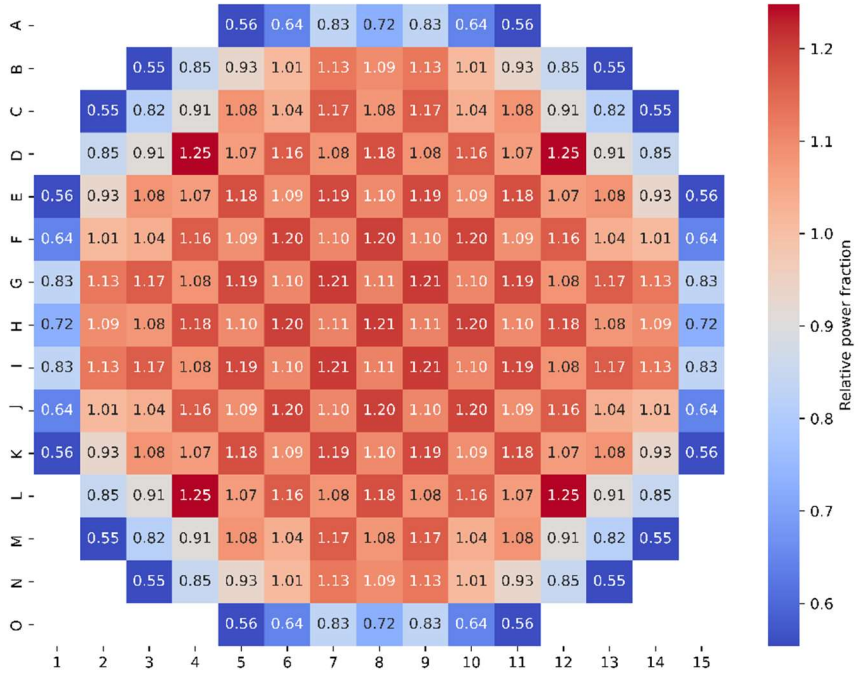

Figure A-26. Radial power profile for Case 5 with PARCS.

A-5. References

[A-1]. Andersen, B. D., "A Machine-Learning Based Approach to Minimize Crud Induced Effects in Pressurized Water Reactors," Dissertation, North Carolina State University, 2021.

[A-2] Quist, D. A., "VERA, Version 1.3, User Manual and Documentation," LA-UR-11-101, Los Alamos National Laboratory, Los Alamos, NM, USA, 2011.

[A-3] ORNL MPACT Team, "MPACT Theory Manual," CASL-U-2019-1874-001, Oak Ridge National Laboratory, Oak Ridge, TN, USA, 2019.

[A-4] Avramova, M. N., and R. K. Salko, "CTF Theory Manual," ORNL/TM--2016/430, Oak Ridge National Laboratory, Oak Ridge, TN, USA, 2016.

[A-5] Smith, K. S., J. A. Umbarger, and D. M. VerPlanck, *SIMULATE-3: Advanced Three-Dimensional Two-Group Reactor Analysis Code User's Manual,* Studsvik Scandpower, Studsvik/SOA-95/15 Rev 2, 1995.

[A-6] Hsien-Chuan, L., Y. Shung-Jung, L. Tzung-Yi, K. Weng-Sheng, S. Jin-Yih, and H. Yu-Lung, "Qualification of the Taiwan power company's pressurized water reactor physics methods using CASMO-4/SIMULATE-3," *Nuclear Engineering and Design*, Vol. 253, pp. 71-76, 2012.

[A-7] Edenius M., K. Ekberg, B. Forssen, and D. Knott, "CASMO-4: A Fuel Assembly Burnup Program User's Manual," Studsvik Scandpower, Studsvik/SOA-95 Rev 1, 1995

[A-8] Bahadir T., J. Umbarger, and M. Edenius, "CCMS-Link User's Manual," Studsvik Scandpower, Studsvik/SOA-97/04 Rev 2, 1999.

[A-9] Hagrman D. T., S. Palmtag, and J. A. Umbarger, "INTERPIN-CS User's Manual," Studsvik Scandpower, Studsvik/SOA-95/21 Rev 1, 2000.

[A-10] Rearden, B. T., and M. A. Jessee, "SCALE Code System," ORNL/TM-2005/39 Version 6.2.3, Oak Ridge National Laboratory, Oak Ridge, TN, USA, 2018.

[A-11] Downar, T. J., D. A. Barber, R. M. Miller, C. H. Lee, T. Kozlowski, D. Lee, Y. Xu, J. Gan, H. G. Joo, J. Y. Cho, K. Lee, and A. P. Ulses, "PARCS: Purdue Advanced Reactor Core Simulator," 2002 International Conference on the New Frontiers of Nuclear Technology: Reactor Physics, Safety and High-Performance Computing (PHYSOR 2002), American Nuclear Society, La Grange Park, IL, USA, 2002.

[A-12] AREVA NP Inc., "Safety Criteria and Methodology for Acceptable Cycle Reload Analyses," Revision 9, BAW-10179NP, Paris, France, 2016.

[A-13] Godfrey A., "VERA Core Physics Benchmark Progression Problem Specifications, Revision 4," CASL-U-2012-0131-004, 29 August 2014, Oak Ridge National Laboratory, Oak Ridge, TN, USA, 2014.

[A-14] Organization for Economic Cooperation and Development Nuclear Energy Agency, "International Fuel Performance Experiments (IFPE) database," Paris, France, 2020. Available at: https://www.oecd-nea.org/jcms/pl_36358/international-fuel-performance-experiments-ifpe-database (accessed 15 August 2022).

[A-15] European Commission – Joint Research Center Institute for Transuranium Elements, "TRANSURANUS Handbook, V1M2J19," Karlsruhe, Germany, 2019.

[A-16] Idaho National Laboratory, "BISON: A Finite Element-Based Nuclear Fuel Performance Code," Idaho Falls, ID, USA, 2022. Available at: https://mooseframework.inl.gov/bison/index.html (accessed 15 August 2022).

[A-17] Idaho National Laboratory, "IFA-431 Rods 1, 2, and 3," Idaho Falls, ID, USA, 1982. Available at: https://mooseframework.inl.gov/bison/LWR/validation/IFA_431/doc/IFA-431.html (accessed 15 August 2022).

[A-18] Idaho National Laboratory, "IFA-650.2," Idaho Falls, ID, USA, 2004. Available at: https://mooseframework.inl.gov/bison/LWR/validation/LOCA_IFA_650/doc/IFA_650_2/IFA_650-2.html (accessed 15 August 2022).

[A-19] Williamson, R. L., G. Pastore, S. R. Novascone, B. W. Spencer, and J. D. Hales, "Modelling of LOCA Tests with the BISON Fuel Performance Code," May 2016, Enlarged Halden Programme Group Meeting, INL/CON-16-37798. Available at: https://inldigitallibrary.inl.gov/sites/sti/sti/7146879.pdf (accessed 15 August 2022).